Effects of High Latitude Light Conditions on Gas Exchange and Morphology in *Trifolium repens*

Rebekka Gullvåg

Thesis submitted for the degree of
Master in Bioscience (Ecology and Evolution)
60 credits

Department of Biosciences
Faculty of Mathematics and Natural Sciences

UNIVERSITY OF OSLO

Spring 2022

Effects of High Latitude Light Conditions on Gas Exchange and Morphology in *Trifolium repens*

Rebekka Gullvåg

Effects of High Latitude Light Conditions on Gas Exchange and Morphology in *Trifolium repens*

http://www.duo.uio.no/

Printed: Reprosentralen, University of Oslo

Abstract

Terrestrial plants play a central role in the Earth system, largely due to photosynthesis and transpiration. Stomata are the gateways that connect the interior of plants with their surrounding atmosphere, regulating both water loss through transpiration and uptake of CO_2 for photosynthesis. Opening and closure of stomata are actively regulated in response to a range of internal and environmental signals, enabling plants to balance this trade-off. Models of vegetation processes, including stomatal conductance, are incorporated in Earth System Models that are used to study the components of the Earth system and climate change.

The unique light conditions at high latitudes include an extended twilight period, characterised by a high proportion of blue light, that can last from sunset until sunrise for parts of the growing season. Plants perceive blue light as a specific signal that regulates many developmental and physiological responses, such as stomatal opening. This thesis investigates how gas exchange, as well as morphological traits, are affected by the extended twilight period at high latitudes in *Trifolium repens* – an agriculturally important species with a broad natural distribution.

Experiments were carried out in controlled growth conditions in order to isolate the effect of low-intensity blue light at night. Three *T. repens* "types" were compared: Two cultivars (Milkanova and Litago), and field-collected individuals from Northern Norway ($\sim$ 69–70°N). The results of this study indicate that the extended twilight at high latitudes has the potential to increase stomatal conductance and affect agriculturally relevant traits. The increase in stomatal conductance did not seem to be accompanied by increased photosynthesis. This may have implications for model representation of agricultural landscapes at high latitudes, which may cover larger areas in the future due to climate change.

Contents

1 Introduction

The waterproof cuticle of vascular plants protects them from desiccation, but also hinders diffusion of CO_2 into the leaves. About 98% gas exchange between a leaf and its surrounding atmosphere occurs through stomata, allowing tight regulation of the trade-off between water loss and CO_2 uptake (Lawson & Blatt, 2014). Stomata are pores between pairs of specialised guard cells in the aerial epidermis of vascular plants ("stomata" is also used collectively for the guard cells and the pores) (Fig. 1). The guard cells integrate environmental and physiological signals and translate this information into changes in stomatal aperture. This regulation enables plants to open stomata in conditions favoring photosynthesis, and close them when water saving is more favorable. Transpiration is also necessary for evaporative cooling of the leaf and is the driving force of the root-to-shoot xylem transport, underpinning the central role of stomatal regulation in plant-water relations. Degree of stomatal opening, in terms of H_2O flux out of the leaf, is referred to as *stomatal conductance* (g_s), and depends on stomatal density and aperture (Lawson & Morison, 2004). There is a tight coupling between stomatal conductance and photosynthetic assimilation (A) (Wong et al., 1979), and stomatal behavior therefore plays a central role in determining water use efficiency (WUE) – the amount of carbon assimilated per unit of water transpired. Throughout this thesis I will consider the *intrinsic* water use efficiency, defined as net photosynthetic assimilation rate (A_n) divided by the stomatal conductance to water vapor (g_s), and refer to this as just WUE.

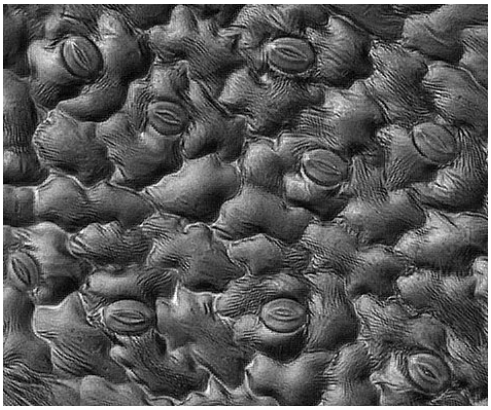

Figure 1: Stomata on the abaxial surface of a *Trifolium repens* leaf. Micrograph of an epidermal imprint. All photos in this thesis are taken by Rebekka Gullvåg.

The gas fluxes through stomata play a central role in the interactions between vegetation and the atmosphere, with implications for the global climate. Plants account for about 60% of global terrestrial evapotranspiration (sum of evaporation and transpiration) (Schlesinger & Bernhard, 2013, p. 401). Furthermore, photosynthesis by terrestrial vegetation is the largest global carbon flux, and has been estimated to 120 Gt carbon per year (Beer et al., 2010). Models of vegetation processes, including stomatal conductance, are included in Earth System Models (ESMs). These are being used to

understand and simulate how different components of the Earth system (land surface, atmosphere, oceans etc.) interact and to study climate change. In this context, there is a need for better understanding and representation of vegetation processes at high latitudes, as there currently is considerable uncertainties associated with model projections in these areas (Rogers et al., 2017). I will focus on the representation of stomatal conductance in the Community Land Model (CLM), which is used in the Norwegian Earth System Model (NorESM2) (Seland et al., 2020). These models are subjects of the EMERALD project (Department of Geosciences, University of Oslo, 2019), to which this thesis is associated. This thesis will investigate the effect of high latitude light conditions on gas exchange and related traits, as well as morphology, in *Trifolium repens* – an agriculturally important species with a broad natural distribution.

1.1 Light Conditions at High Latitudes

The light conditions at high latitudes constitute a unique growth environment. There is an extreme seasonal variation in photoperiod, but the low solar altitude angle also affects the spectral composition of daylight. Due to an increased pathway through the atmosphere, there is more scattering and therefore the proportion of diffuse light is increased. In effect, the light is enriched in the blue region of the spectrum, as short wavelengths are most prone to scattering (particularly Rayleigh scattering) (Smith & Morgan, 1981). This is especially pronounced during twilight, when the sun is $0 - 18^{\circ}$ below the horizon and diffuse light is the only light source. There is also a slight increase in the proportion of far-red light at twilight (Smith & Morgan, 1981). Duration of the twilight period is determined by latitude and season, and increases with latitude (except for periods with polar day or night above the Arctic/Antarctic circle). Above about 50°N/S, twilight lasts continuously from sunset to sunrise for parts of the growing season (Boggs, 1931). As stomatal regulation, as well as many other physiological and developmental processes in plants, are sensitive to blue light (see section 1.2.1), they may be affected by the extended twilight period found at high latitudes.

1.2 Stomatal Regulation by Light

The volume and turgor pressure of the guard cells determine the size of the stomatal pore. Specialised cell wall structures cause the guard cells to bow outwards when volume increases due to water-influx, resulting in increased stomatal aperture. As a consequence, gas exchange between the leaf and its surrounding atmosphere increases. Guard cell volume is tightly regulated by a complex network of responses to internal and external signals (Assmann, 1993). The signals are integrated in the guard cells, resulting in an appropriate response, allowing the plant to regulate the balance between CO_2 uptake and transpiration in relation to the ambient conditions. Generally, stomata are open during the day and closed at night in C_3 and C_4 plants, preventing excessive water loss when there is no CO_2 fixation. Light, low CO_2 concentration in the leaf, low vapour pressure deficit, and high temperature promote stomatal opening (Matthews & Lawson, 2019), while the contrary of these factors, as well as drought, promotes closure. In addition, endogenous factors and circadian rhythms are involved in stomatal regulation. This section will focus on stomata regulation in relation to light conditions, particularly focusing on the effects of blue light.

1.2.1 Light-induced stomatal opening

In temperate conditions, the principal stimulus promoting stomatal opening is light (Zeiger, 2018). There are two main mechanisms in light induced stomatal opening: 1) an indirect effect of photosynthesis driven by PAR (photosynthetic active radiation, mainly by red and blue light), also referred to as "the red light response"[1], and 2) a specific response to blue light (Zeiger & Field, 1982). Responses two to 20 times more efficient to blue light than to red light alone, given equal energy levels, have been reported (Willmer & Fricker, 1996, p. 133). Also, an enhanced response has been observed when blue light is superimposed on a red-light background, suggesting a synergistic effect (Karlsson, 1986). However, dependence on red light for the blue light response varies among species, with some responding to low-intensity blue light alone, while others respond to blue light only when combined with red light (Matthews et al.,

[1]The PAR driven stomatal response is often referred to as "the red light response" because dual beam experiments with red and blue light often are used to study the two responses. By saturating the PAR response with red light before applying weak blue light, the specific guard cell response to blue light is isolated (as blue light also is a part of PAR) (see e.g. Karlsson, 1986).

2020). Moreover, the sensitivity to blue and red light may be affected by growth conditions (Matthews et al., 2020). Although blue light induced stomatal opening has been observed in several species, it is not universal and knowledge about diversity in blue light responsiveness is sparse (Matthews et al., 2020). Nevertheless, the blue light response is thought to have an important functional role in certain conditions, as it is rapid and highly sensitive to low intensities (Zeiger et al., 1981; Zeiger & Field, 1982).

The specific blue light response of stomata

Blue light induces stomatal opening by acting as a specific signal perceived by the photoreceptors, phototropins, in the guard cells (Kinoshita el al., 2001). Isolated guard cell protoplasts swell upon blue light irradiation, showing that all signaling components in blue-light-induced opening are contained within the guard cells (Zeiger & Hepler, 1977). Blue light absorption by the phototropins initiates a signalling pathway resulting in activation of a plasma membrane H^+-ATPase (Inoue et al., 2010; Kinoshita & Shimazaki, 1999), that causes hyperpolarization of the plasmamembrane (Assmann et al., 1985). This activates voltage-gated K^+ channels, as well as other osmoregulatory mechanisms, resulting in the accumulation of ions in the guard cells (Schroeder et al., 1987; Talbott & Zeiger, 1996). The resulting decrease in guard cell water potential causes water influx, and the stomatal pore opens as the guard cells swell.

1.3 Water Use Efficiency – Coordination of g_s and A_n

There is often a strong correlation between stomatal conductance (g_s) and photosynthetic rate (A_n) (Brodribb et al., 2020). In fact, selection for increased yield has in many cases inadvertently resulted in increased g_s in modern crops (Roche, 2015). The stomatal aperture determines the availability of CO_2 for photosynthetic fixation, and g_s is in turn affected by the photosynthetic activity in the leaf (Wong et al., 1979). Several mechanisms are involved in this coordination, including circadian regulation of stomata, guard cell responses to $[CO_2]$ inside the leaf and the concentration of photosynthate, as well as parallel responses to environmental factors – such as light (Gago et al., 2016; Matthews & Lawson, 2019). The tight coupling between A_n and g_s is thought to have a functional role in balancing carbon uptake against water saving, and seems to be common across vascular plant lineages (Brodribb et al., 2020; Cowan & Farquhar, 1977).

Slow responses in g_s can limit A_n, while high g_s can increase A_n at the expense of WUE (Lawson & Vialet-Chabrand, 2019). Upon changes in environmental factors, responses in g_s are in general considerably slower than responses in A_n. As a result of this asynchrony, WUE is often sub-optimal in dynamic environments. Mismatch between g_s and A_n may also occur when a plant is subject to conditions that affect g_s and A_n to different degrees.

1.3.1 The Stomatal Blue Light Response and WUE

The specific blue light response of stomata is highly sensitive, and is therefore capable of causing stomatal opening in response to quantum fluxes too low to drive photosynthesis (and thus photosynthesis dependent stomatal opening) (Zeiger & Field, 1982). Zeiger and colleagues (1981) demonstrated that stomatal opening at pre-dawn, before the light compensation point of photosynthesis is reached, is a specific response to blue light. The authors suggested this to be an adaption to the light quality at dawn (enriched in blue light), which according to their calculations maximises carbon assimilation in the early morning (especially in water-limiting conditions). On the other hand, blue light enhances stomatal opening even after photosynthesis is saturated in some species (Shimazaki et al., 2007; Matthews, 2020). This suggests that blue light induced stomatal opening in some cases reduces WUE by increasing stomatal conductance even when CO_2 assimilation has reached its maximum. The effect blue light induced stomatal opening has on carbon assimilation, is determined by whether (and to what extent) photosynthesis is limited by CO_2 diffusion into the leaf (Matthews et al., 2020). So while the blue light response may reduce WUE when photosynthesis is saturated, it may increase photosynthetic assimilation by alleviating CO_2 limitation in the morning.

Blue light also acts as a specific signal in many developmental processes in plants (Christie, 2007; Huché-Thélier et al., 2016), and may therefore affect morphological traits. For instance, blue light can affect growth pattern and leaf characteristics (Huché-Thélier et al., 2016). The effects blue light may have on plant productivity and WUE are interesting in the context of crop production and at high latitudes, but also for models of stomatal behaviour–which often assume optimal WUE (Buckley, 2017).

1.4 Representation of Stomatal Conductance in Land Surface Models

Vegetation plays a central role in the terrestrial hydrological and carbon cycles, through transpiration and photosynthesis, respectively. Moreover, transpiration influences surface energy balance by contributing to latent heat flux, which cools the surface. As stomatal behaviour regulates both transpiration and photosynthesis, a sound representation of g_s is needed in modelling of land surface processes (Buckley, 2017). Models of g_s at the leaf-scale can be scaled to estimate canopy conductance in Land Surface Models (LSMs), which are used as the terrestrial component in Earth System Models (ESMs) (Bonan, 2016, p. 280 ; Franks et al., 2018).

Empirically/phenomenologically based stomatal conductance models have been widely implemented in ESMs (Franks et al., 2018). More recently however, increasing attention has been paid to g_s models based on optimal stomatal conductance theory – assuming that stomata act to maximise WUE (Medlyn et al., 2011). Two now widely used g_s models are the Ball-Berry model (Ball et al., 1987) and the Medlyn model (Medlyn et al., 2011)(Franks et al., 2018). These are the two current alternatives in FATES (Functionally Assembled Terrestrial Ecosystem Simulator) – a dynamic vegetation module which can be run with the Community Land Model (CLM) as "Host Land Model" (Lawrence et al., 2018).

The Ball-Berry and the Medlyn model both represent g_s as a function of A_n, with A_n estimated by the Farquhar-Caemmerer-Berry photosynthesis model (Ball et al., 1987; Farquhar et al., 1980; Medlyn et al., 2011) (see Appendix A.1 for model details). The equations for A_n and g_s are solved iteratively in a coupled photosynthesis-conductance leaf model. Mathematically, the two g_s models have a similar structure. While the Ball-Berry model uses empirically estimated relationships between g_s and A_n, the Medlyn model is directly derived from WUE optimalization theory (Medlyn et al., 2011). However, the Ball-Berry model is also consistent with the optimality assumption (and as WUE is the ratio A_n/g_s, the estimated relationship between g_s and A_n contains information of the plants' WUE) (Franks et al., 2017; Medlyn et al., 2011). The two models have indeed been found to have equal predictive strengths, except for in conditions of extremely dry or humid air (Franks et al., 2017; Franks et al., 2018).

Common to the two models is also that light is only included indirectly, through its effect on photosynthesis (Ball et al., 1987; Medlyn et al., 2011). PAR incident on the leaf is used to calculate the light-limited rate of photosynthesis, which can determine A_n in the Farquhar-Caemmerer-Berry photosynthesis model (Lawrence et al., 2018). Light is here included in terms of energy (W/m^2) available for photosynthesis. As described in Section 1.2, there are two main mechanisms of stomatal regulation by light: The indirect effect of PAR, driving photosynthesis, and the specific blue-light response of the guard cells. These models of stomatal conductance only consider the indirect effect of PAR, not the specific response to blue light. The higher proportion of blue light at high latitudes might increase the relative importance of the stomatal blue light response, and thus potentially also result in sub-optimal WUE. If so, the assumptions of widely used g_s models might be less representative of vegetation at high latitudes.

1.5 Study Species: *Trifolium repens*

White clover (*Trifolium repens* L.) is considered the most important pasture legume in the temperate zone (Frame & Newbould, 1986). It is mainly grown in mixed swards with grasses, and reduces the demand for fertilizer due to the symbiosis with nitrogen-fixing *Rhizobium* bacteria. It is also a highly valued fodder crop because of its high nitrogen content and digestibility compared to grass species (Frame & Newbould, 1986).

T. repens has a wide natural distribution in northern Eurasia, but is introduced and naturalized in America and Oceania and has now a cosmopolitan distribution (Global Invasive Species Database, 2010). Accordingly, the species inhabits a wide range of latitudes and climatic conditions. In Norway, it is common up to 70°N (Aasmo Finne et al., 2000). In contrast to other legumes of agricultural interest, northern populations of *T. repens* have the capacity to withstand harsh winters (Aasmo Finne et al., 2000). *T. repens* therefore has a large potential for agriculture in regions such as northern Scandinavia.

Effort has been made in developing cultivars suitable for northern climatic conditions. One of these is Litago, developed by Graminor, which currently is the most used white clover cultivar in Norway (Graminor, n.d.). In this project I will compare Litago to the Danish cultivar Milkanova, which has been considered a "standard market cultivar"

(Aasmo Finne et al., 2000) and is included here as a "southern" cultivar. These cultivars will be compared to field-collected (wild) individuals from Finnmark (at $\sim 69 - 70$°N), which will be referred to as "Finnmark".

1.6 Research Questions

This thesis will investigate the effects of an extended twilight period ("high latitude light conditions") on gas exchange and related traits in the three *Trifolium repens* types: Finnmark, Litago and Milkanova. My specific research questions are:

1. Is plant gas exchange through the diurnal cycle affected by the extended twilight period?
2. Do high latitude light conditions induce morphological changes in *T. repens*?
3. Do the selected *T. repens* types differ in their responses to high latitude light conditions?
4. Do high latitude light conditions affect traits relevant to Earth System Modelling?

2 Materials and Methods

2.1 Plant Material

Wild individuals collected in Finnmark (Northern Norway) and two cultivars of *Trifolium repens* were used for this study, referred to as three types: Finnmark, Litago and Milkanova. The Finnmark plants had been collected for a previous project, during the late summer and autumn of 2017 and 2018 (Appendix, Table A.1). The cultivars were grown from commercial seeds (Litago, Strand Unikorn AS, Moelv, Norway; Milkanova, Leüthens Frø AS, Trondheim, Norway). Seeds were broadcasted on a 10:1 mixture of peat-based potting soil (P-Jord, Tjerbo Torvfabrikk AS, Norway) and perlite (Perlite agra grade, LOG AS, Oslo, Norway) in plastic trays. After ten days, groups of about 10 - 50 seedlings were transferred to plastic pots (10 cm diameter), eight pots for each type. After an additional 26 days, 18 individual plants of each type were separated and transferred to individual pots (9 cm diameter).

Two experiments, with the same experimental treatments, were conducted: *Experiment 1* and *Experiment 2* (Fig. 2). The second experiment was needed as the diurnal measurements were delayed (due to technical issues with the measuring instrument). Experiment 1 was carried out April - May 2021, and Experiment 2 was carried out October - December 2021. Prior to each experiment, stem cuttings were taken from the plants, assuring that they were of similar (and convenient) size at the beginning of the experimental treatment. For Experiment 1, six cuttings (clones) of nine individual plants (genotypes) were included for each type, divided between the two light treatments (81 in total per treatment). For Experiment 2, three genotypes per type were included. Two clones per genotype were prepared for each light treatment. However, due to time-limitation only one clone per genotype was measured in each treatment (9 in total per treatment). In all cases, only leaves developed after onset of the experimental treatment were sampled (this was kept track of by marking young petioles with permanent marker by the start of the treatment).

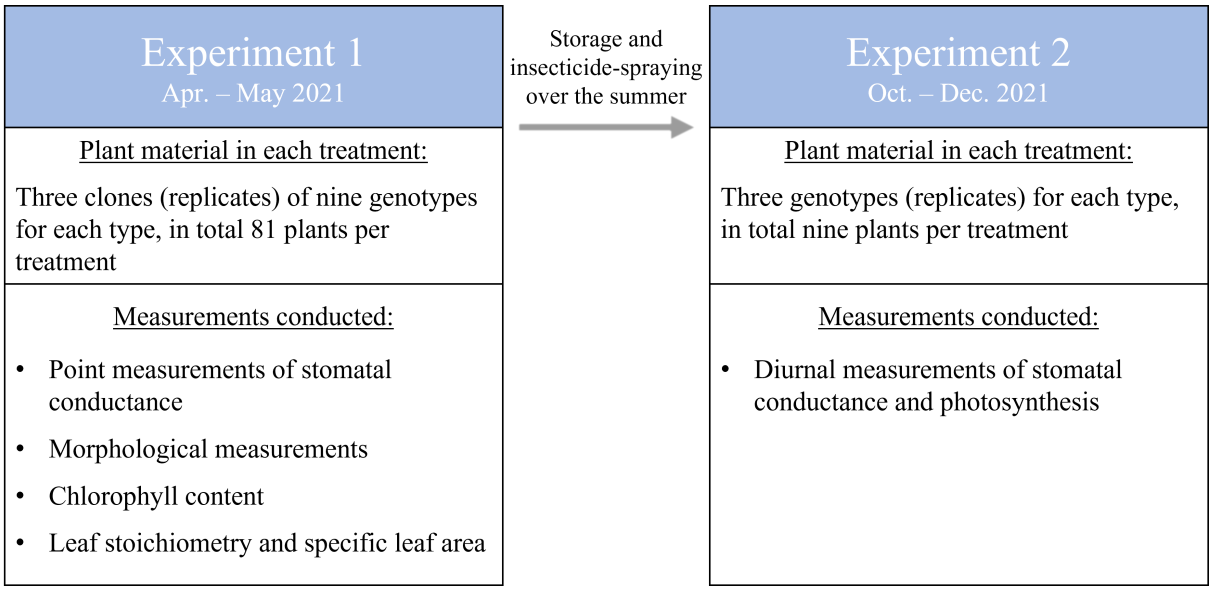

Figure 2: Flowchart of the experiments. Two experiments with the same experimental treatments were conducted. Three "types" of *Trifolium repens* were used: Wild individuals collected in Finnmark, and two cultivars – Litago and Milkanova. Number of plants per treatment given here are those used for the actual measurements. For some of the analyses in Experiment 1, only a sub-sample was used.

Stem cuttings included the stolon apex and four additional nodes. All leaves, except the youngest, were removed. The cuttings were rinsed in tepid soap water (Zalo, Orkla ASA, Ski, Norway), in order to eliminate thrips (see section 2.2.3). Each cutting was planted in an individual plastic pot (9 cm diameter for Experiment 1, 12 cm for Experiment 2), filled with peat-based potting soil and perlite (mixed 10:1 (P-Jord, Tjerbo Torvfabrikk AS, Norway; Perlite agra grade, LOG AS, Oslo, Norway)), so that three nodes were covered. The newly planted cuttings were thoroughly watered and covered with a transparent plastic sheet, keeping them moist. They were left to establish in a climate controlled phytotron room (10 m^2), with a 18 h photoperiod, using high intensity discharge lamps (400 W Powerstar HQI-BT daylight, OSRAM, Germany) as light source. Except for light conditions, growth conditions were the same as during the experiments (see following section).

2.2 Growth Conditions and Experimental Set-up

2.2.1 Growth Conditions

In order to isolate potential effects of light conditions, the experiments were conducted in controlled growth conditions in the Phytotron at the University of Oslo. Half of the

clones of each genotype were grown in one of two climate controlled phytotron rooms (10 m^2). Except for light condition (details in subsequent section), all environmental factors were kept as equal as possible in the two rooms: Temperature was set to 20°C (precision ±1°C); humidity was set to 60%, with a precision of approximately ±10% (measurements showed an average humidity of about 68%); plants in both rooms were watered daily, and fertilised weekly, with a mixture of 2 ‰YaraTera Kristalon Indigo (NPK 9-5-25 +Mg-S-micro, Yara AS, Norway) and 0.5 ‰YaraTera Calcinit (NPK 15.5-0-0 +Ca 19.0%, Yara AS, Norway). However, half-way through Experiment 2 the plants showed symptoms of nutrient-deficiency, and were therefore fertilised twice a week for the remainder of the experiment. They were also transferred to larger pots (1.5 L), to avoid drying between each watering. The plants were rotated weekly to reduce confounding effects due to environmental gradients in the rooms.

2.2.2 Experimental Design and Light Treatment

Two light treatments were compared in the experiments: A high-latitude light treatment (HL) and a low-latitude light treatment (LL). Both rooms had a 18 h day with white growing light. For the night, the HL light treatment had 6 hours of "twilight" represented by weak blue light, while the LL light treatment 30 min of twilight during the first and last 30 min of the night, and darkness for 5 h (Fig. 3). The light source for the white growing light was high intensity discharge lamps (400 W Powerstar HQI-BT daylight, OSRAM, Munich, Germany). This should have given a photosynthetic photon flux density (PPFD) of 200 µmol photons m^{-2} s^{-1} ± 10% at plant height, with the spectral distribution shown in Figure 4, in both rooms. However, when light measurements were done at the end of Experiment 2, the day light intensity was unfortunately different in the two rooms: 222 ± 18.5 µmol photons m^{-2} s^{-1} in HL, and 178 ± 12.4 µmol photons m^{-2} s^{-1} in LL.[2] This difference was confirmed by the light measurements that were logged automatically during the diurnal gas exchange measurements (Section 2.3.2), but was not evident in the test-runs of the diurnal gas exchange measurements that were conducted during Experiment 1. Presumably, lamp changing occurred in the HL room during the summer, without my knowledge. I therefore assume that the light conditions during the day were equal in the two

[2]Mean and standard deviation of measurements at plant height (measured by Ane V. Vollsnes, using an LI250 with an LI190R quantum sensor (LI-COR Biosciences, Lincoln, NE, USA))

treatments during Experiment 1, although it was a source of error during Experiment 2.

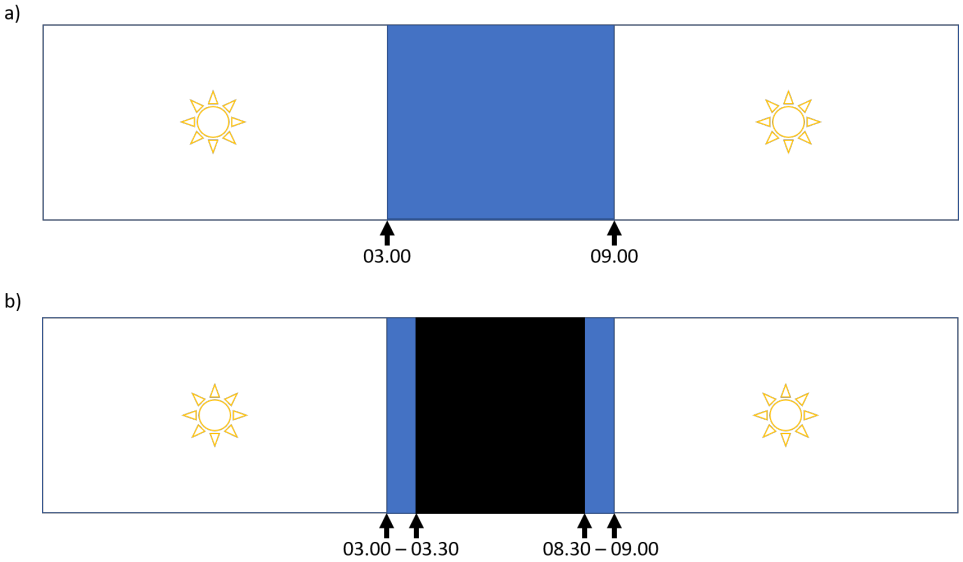

Figure 3: Illustration of experimental light conditions over 24 h in the two phytotron rooms. The white areas represent day with white growing light, the blue areas represent twilight with only weak blue light, and the black area represents darkness. **a)** High-latitude light treatment (HL): 18 h day, and 6 h twilight. **b)** Low-latitude light treatment (LL): 18 h day, twilight during the first and last 30 min of the night, and darkness for 5 h.

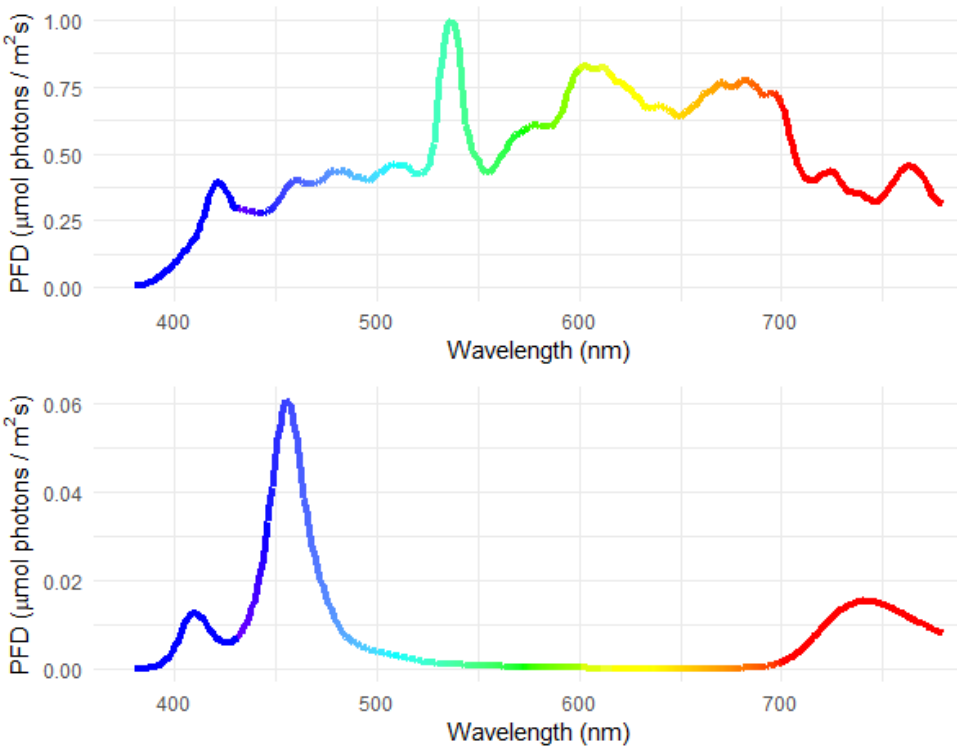

Figure 4: Spectral distribution of light in the phytotron rooms, measured at plant height with an MK350S Premium Spectrometer (Gamma Scientific, San Diego, CA, USA). The upper panel shows the white growing light, while the lower panel shows spectral distribution of the LEDs with blue filters that were used to mimic twilight. Note the different scales. PFD = Photon flux density.

For the artificial twilight, two LED tubes (L28-120 NS12, Valoya, Helsinki, Finland) were covered with blue filters (GamColor® 855 (no. BRU-GAM-F0855), Blue Jazz, Norsk Sceneteknikk AS, Spydeberg, Norway) and hung up 61 cm above plant height in both rooms (Fig. 5). These gave a weak blue light, with the spectral distribution shown in Figure 4 and a PPFD measured to 1.5 ± 0.4 µmol photons m^{-2} s^{-1} at plant height. The LEDs were controlled by a timer, according to the time scheme shown in Figure 3. In the HL treatment, the weak blue light was on for the entire night. While in the LL treatment, the blue light was on only the first and last 30 min of the night, mimicking dawn and dusk.

Figure 5: Experimental set-up at the beginning of Experiment 2. Twilight was mimicked by two LED tubes covered with blue filters. As the *Trifolium repens* grew larger, the pots were distributed on two tables.

2.2.3 Pest Control

During Experiment 1 (Spring 2021), plants in both rooms were infested with thrips (order Thysanoptera). In order to limit the infestation, they were sprayed with the insecticides Conserve SC (Dow AgroSciences, Zionsville, IN, USA) and Decis Options (Bayer AG, Leverkusen, Germany) prior to the experiment (Table A.2). Furthermore, cuttings were rinsed in tepid soap water (Zalo, Orkla ASA, Ski, Norway) during propagation. For all measurements and sampling, damaged leaves were avoided as far as possible. When Experiment 1 was completed, new cuttings were taken (as described in Section 2.1). These were stored over the summer and repeatedly sprayed with Vermitec (Syngenta, Basel, Switzerland) and Decis Options (Table A.2), resulting in the elimination of thrips before Experiment 2.

2.3 Gas Exchange Measurements

Two sets of gas exchange measurements were conducted. During Experiment 1, point measurements of stomatal conductance (g_s) were taken using an AP4 porometer

(Delta-T Devices, Cambridge, UK). Secondly, stomatal conductance and net photosynthetic rate (A_n) were measured continuously through the diurnal cycle during Experiment 2, using an LI6400 Portable Photosynthesis System (LI-COR Biosciences, Lincoln, NE, USA). The AP4 porometer operates by measuring the rate of which relative humidity increases in a cup chamber below the leaf surface, thereby measuring only one side of the leaf. As the plants used for these experiments were amphistomatous (having stomata on both leaf surfaces), and the stomatal ratio seemed to vary, both leaf surfaces were measured. In contrast, LI6400 calculates total g_s and A_n per leaf area, and was used with a leaf chamber containing a larger part of the leaf. A_n and g_s are calculated based on differences in CO_2 and H_2O concentrations in the leaf chamber compared to reference air by-passing the sample. These concentrations are measured by infrared gas analysers (IRGAs). Another central difference between LI6400 and the porometer, is that conditions in the leaf chamber of LI6400 may be actively regulated. LI6400 also allows for automatic measuring series, and could therefore be used to make 24 h continuous measurements in this project.

2.3.1 Point Measurements of Stomatal Conductance

Stomatal conductance was measured in four time intervals, spaced throughout the day, using the AP4 porometer (Delta-T Devices, Cambridge, UK). The measurements were conducted over the course of six weeks (April - May 2021, Experiment 1), in a random order. Due to time limitation, only one clone of each genotype was included. This resulted in nine measurements for each type in both treatments, in each of the time intervals: 08:30 – 09:00, 09:00 – 10:00, 11:30 – 13:00, and 16:00 – 17:00. The first interval, 08:30 – 09:00, represents dawn, with weak blue light in both rooms (Fig. 3). The first hour after white "daylight" was turned on constitutes the second time interval, while the two remaining intervals make up mid-day intervals.

Stomatal conductance was measured on both sides of one leaflet for each plant. Well-lit, undamaged, and fully developed leaves (third or older counting from the apical bud) were selected for the measurements. The leaflet midrib and damages were avoided as far as possible. The abaxial side was measured first. As stomatal ratios (fraction of conductance on one side of the leaf to the other) varied, the sums of adaxial and abaxial stomatal conductance were used for further analysis.

2.3.2 Diurnal Measurements of Stomatal Conductance and Photosynthesis

Diurnal measurements of stomatal conductance (g_s) and net photosynthetic rate (A_n) were conducted during Experiment 2, using the LI6400 Portable Photosynthesis System (LI-COR Biosciences, Lincoln, NE, USA) and automatic logging with *AutoLog2*, one of the pre-installed standard *AutoPrograms*. The measurements were often unstable for the first 30 – 60 min, therefore, the AutoProgram was run for 25 – 26 h to obtain 24 h measuring series. Flow rate was set to 500 µmol s^{-1}, reference CO_2 to 400 ppm, and block temperature to 20°C. The desiccant tube knob was set close to full bypass, and the desiccant (Drierite) was exchanged between every measurement. Logging was based on stability (using the default stability definition), so that the instrument waited for stability for minimum 60 s and maximum 90 s before logging. Matching (between the sample and reference IRGAs) was done every 30 min. These settings, and the following set-up, were determined after extensive trial and error.

The set-up for the diurnal measurements is shown in Figure 6. An external 40 L cylinder (containing >99% CO_2) was used as CO_2 source. The sensor head was placed on a table next to the watering table, at the same height. The plant could then stay on the watering table, under the blue LEDs, during the measurement (the same spot was used every time). One undamaged, mature leaf (at least number three counting from apex) was placed in the leaf chamber for each measurement. A standard 2x3 cm chamber was used for the final measurements. To keep the leaf flat and in place, in spite of nyctinastic movements, pieces of fishing line were taped onto the inner edges of the foam gaskets lining the chamber (Fig. 7).

The pot with the plant being measured was placed in a plastic tray with water, to avoid drying during the measurement. However, the humidity in the phytotron room peaked after watering, before a measurement was started, and then fell slowly throughout the measurement. To obtain a less humid and variable intake air, a flexible plastic tube, connected to the air inlet of the instrument, was slid under the door sweep and hung up in the hallway outside the phytotron room.

Leaf area had to be determined manually, as the leaves did not completely cover the leaf chamber. This was done by stereological point counting. Before each diurnal gas exchange measurement, the leaf inside the chamber was photographed. A grid of crosses 3 mm apart was superimposed on each image, and the crosses of which the center hit the leaf was counted (Fig. 7). Leaf area was estimated by multiplying the point count by the squared grid size. The analysis was conducted using Fiji software (Schindelin et al., 2012).

Figure 6: Set-up for the diurnal measurements of *Trifolium repens*, using an LI6400 portable photosynthesis system. A 40 L gas cylinder was used as CO_2 source, and air from outside the phytotron room was conveyed through a plastic tube to the air intake of the instrument. During the measurements, the plant pot stood in a plastic tray with water on the watering table, while one leaf was held in the LI6400 sensor head (with a standard 2x3 cm leaf chamber) on an adjacent table.

The final measurements were collected within eight weeks during October - December 2021, in a random order. Due to various technical and practical issues, at least two attempts were needed for most of the measurements. For instance, recurring problems with CO_2 regulation and temperature measuring in the instrument resulted in delays. Faulty temperature measurements were later found to be caused by damaged insulation around a wire leading to one of the temperature sensors. Due to time-limitation, only three genotypes per white clover type were included, with one measurement each (in both rooms), 18 in total.

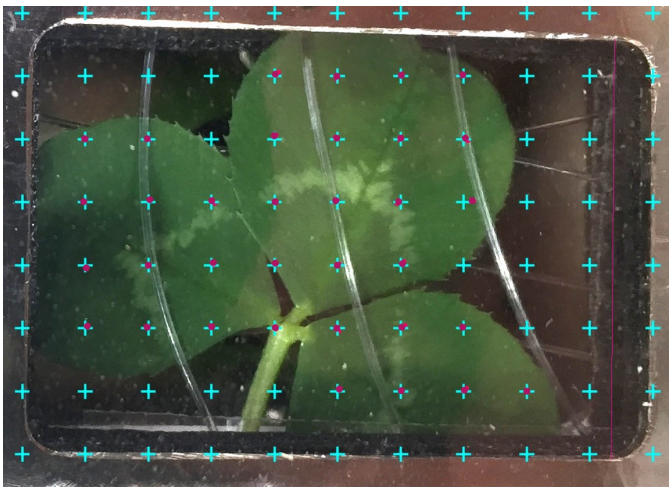

Figure 7: Example of a *Trifolium repens* leaf in the LI6400 standard 2x3 cm chamber, with a 3 mm grid used to determine area. The counted points are marked by pink dots. The scale is set after the chamber by the vertical pink line (2 cm). Fishing line was used to keep the leaf in place.

2.4 Leaf Blade Composition

2.4.1 Chlorophyll Content

Chlorophyll Content Measurements

Chlorophyll content was measured using an Opti-Sciences (Hudson, NH, USA) Chlorophyll Content Meter, CCM-300, on one leaflet blade per plant at the end of Experiment 1. All 162 plants were included (Fig. 2). Leaves were chosen after the same criteria as for the porometer measurements.

CCM-300 measures chlorophyll content based on the fluorescence emission ratio at 735 nm/700 nm (based on Gitelson et al. (1999)). To relate CCM-300 output values to absolute values of chlorophyll content in *T. repens*, chlorophyll content was additionally measured by chemical analysis for a sub-sample of leaves (see following subsections). The relationship between the two units was determined through linear regression. The resulting standard curve (Fig. 8) was used to convert all CCM-300 measurements to absolute chlorophyll content per leaf area.

Chlorophyll a Standard Curve: Samples

Chemical analysis of chlorophyll content was conducted using a microplate reader (Synergy™ Mx, BioTek Instruments Inc., Winooski, VT, USA). Leaf blade samples were collected from three Litago genotypes, three Milkanova genotypes and four Finnmark genotypes (two from two different locations)[3], with three replicates from each genotype. After measurement with CCM-300, the measured part of the blade was cut loose (whole leaflet blades were used for the smallest leaves). The samples were photographed on red millimetre paper, and their areas were later determined using colour threshold, and adjusting manually, in Fiji software. The samples were stored in individual Eppendorf tubes at -80°C.

Chlorophyll a Standard Curve: Chlorophyll Extraction

The samples were transferred to individual 1.5 mL VWR screw cap microcentrifuge tubes (article no. 525-0647), after thawing for about ten minutes. 1.4 mL 96 % ethanol was added to each tube. The tubes were shaken and then vortexed for about ten seconds. The samples were covered with aluminium foil for dark extraction and placed

[3]Karasjok and Øvre Neiden (Table A.1)

in a refrigerator at 4-5°C for 48 hours. To assess whether sample size affected the extraction, chlorophyll content was later plotted against the area of the leaf sample from which it was extracted. No correlation was found between sample size and chlorophyll content (Fig. A.3).

Chlorophyll a Standard Curve: Dilution and Analysis

The sample extracts were 20-fold diluted: 950 µL 96 % ethanol was added in 30 new 1.5 mL screw cap microcentrifuge tubes, and 50 µL from each sample was added to individual tubes. The tubes were shaken, and three samples of 250 µL from each diluted sample were added to wells on a Falcon® 96-well Clear Microplate (resulting in three repeated measurements for each replicate – averages of the repeated measurements were used for the standard curves). This volume and dilution factor was found to be suitable for these samples by a preliminary test with the microplate reader.

In order to convert output values from the microplate reader to absolute chlorophyll a concentration, Sigma-Aldrich Chlorophyll a analytical standard, article no. 96145 (0.1 mg chlorophyll a/mL) was used to make a standard curve (Fig. A.1). The chlorophyll standard was diluted with 96 % ethanol: 300 µL standard was added to 3 mL ethanol, and this was repeated in series four times. Calculations and exact concentrations are shown in Appendix section A.4.1. Three samples of 250 µL from each dilution step were added to wells. Additionally, 250 µL 96 % ethanol was added to three wells as blanks. All sample measurements, for which this standard curve (Fig. A.1) was used, fell well within the concentration range of the standard curve (Appendix Table A.3).

Absorbance was measured at ex/em at 460/680 nm with the microplate reader. Also, in order to assess potential differences in pigment composition, absorption spectra were constructed by measuring absorbance at wavelengths from 350 nm to 750 nm. Chlorophyll a and b concentrations were calculated after Lichtenthaler (1987, p. 366), using the equations:

$$C_a = 13.36A_{664} - 5.19A_{649}$$

$$C_b = 27.43A_{649} - 8.12A_{664}$$

where C_a and C_b are the chlorophyll a and b concentrations in the wells, while A_{649} and A_{664} are the absorbances at 649 nm and 664 nm, respectively. The ratio C_a/C_b for each

replicate (calculated from averages of the repeated measurements) was used to compare the three *T. repens* types. Complete overlap was found among the three types (see appendix, Fig. A.4), and the three types are therefore assumed not to differ in C_a/C_b at a level that is relevant for the assumptions made here.

Chlorophyll a Standard Curve for *T. repens*

The relationship between absolute chlorophyll content, determined using the microplate reader, and CCM-reads (for the same leaf samples) was determined through linear regression (Fig. 8). The chlorophyll a concentrations in the wells were first converted to content per leaf area (µg/cm^2), by multiplying with the dilution factor and extraction volume, and dividing by the leaf sample area. The resulting linear relationship: $y = 0.1872x - 9.4047$ ($R^2 = 0.5226$) (Fig. 8), was used to convert all CCM-reads to absolute units of chlorophyll concentration per leaf area. Accordingly, one common model was applied on all three types. Separate models for each type were tested, but could not be shown to differ at any relevant level of significance (Appendix Fig. A.5 and Table A.5). As the CCM-300 measures both chlorophyll a and b, while only a chlorophyll a standard was used for the chemical analysis, differences in C_a/C_b ratios could potentially affect the relationship between the two measuring techniques. Therefore, the overlap found in C_a/C_b is an argument for a common model.

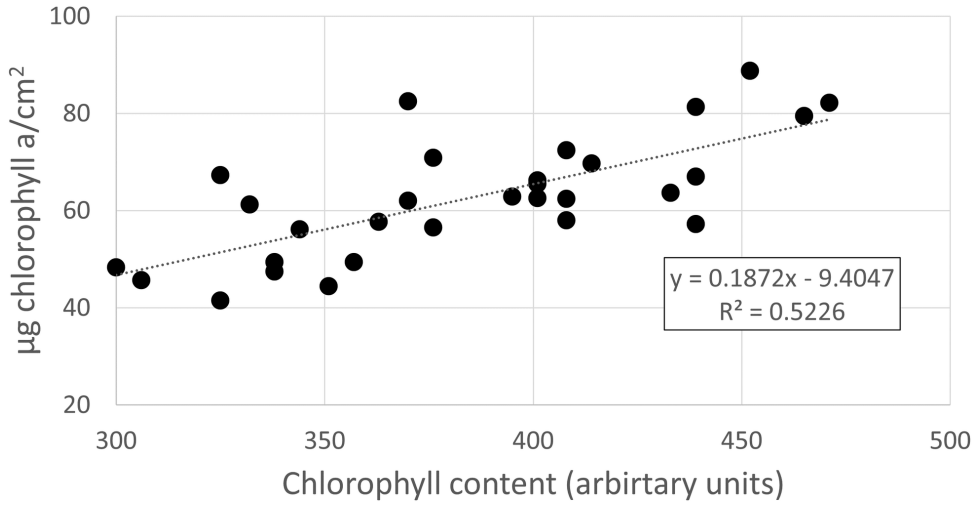

Figure 8: Standard curve relating chlorophyll content measured with CCM-300 (arbitrary units) to chlorophyll a content per leaf area in *Trifolium repens*. Chlorophyll content was measured with a CCM-300 for every clone at the end of Experiment 1, and was converted to chlorophyll content in µg/cm^2 by this linear model (y = 0.1872x − 9.4047).

2.4.2 Leaf Blade Stoichiometry and SLA

Specific leaf area (SLA, the ratio of leaf area to dry mass) and leaf stoichiometry, particularly leaf nitrogen content, are closely related to photosynthetic rates and stomatal conductance (see e.g. Meziane & Shipely, 2001; Walker et al., 2014). In this project, SLA as well as the content of nitrogen (N) and carbon (C) in leaves were analysed for a sub-sample of the genotypes. Three genotypes per type were included, each with one clone from each light treatment. Leaf samples were collected at the end of Experiment 1. One healthy and mature leaf (at least number three from apex) was collected from three genotypes of each type in both treatments. These were the same plants that were used to make epidermis imprints (section 2.5.2). The leaves were cut loose at the base of the trifoliate leaf blade. Each blade was photographed on red millimeter paper, and area was later determined from the images, using colour threshold in Fiji software. Fresh weight was measured, and blades were placed in aluminium foil envelopes and left to dry at 105°C for three days. Dry weight was noted for calculation of SLA.

The dry leaf samples were later used to analyse N and C content. For each sample, one leaflet was weighed into tin capsules for analysis with a Flash EA 1112 NC Analyser (Thermo Fisher Scientific, Waltham, MA, USA). The method is based on Dynamic Flash Combustion, where the sample is completely combusted and the resulting elemental gases are chromatographically separated and quantified by a thermal conductivity detector. The ratio of N/C content was used for further analysis.

2.5 Morphological Measurements

2.5.1 Plant Growth and Architecture

Several measurements on plant growth and architecture were conducted after eight weeks in the experimental light treatments (at the end of Experiment 1; Table 1). All 162 plants were included (Fig. 2). Length measurements were done using a plastic ruler. Squared leaflet vein length was used as a proxy for leaflet area, as there was a strong positive relationship between these two measurements (Fig. A.2). Due to practical limitations, the morphological measurements were taken over the course of three weeks, which likely contributed to the observed variation in maximal stolon length and number

of internodes on the longest stolon. However, as the order of the measurements were random, this was assumed not to produce consistent bias in the results.

Table 1: Overview of morphological measurements conducted at the end of Experiment 1, and the criteria applied.

Measurement	Criteria	Trait of Interest
Leaflet vein length (cm)	Measured on the middle leaflet of the sixth leaf counting from apex, only including leaves that had emerged from the stipules. This was repeated on three branches on each plant. If the sixth leaf was damaged, the seventh was measured.	Leaflet size
Petiole length (cm)	Measured on the same leaves as leaflet vein length.	Petiole elongation
Maximal stolon length (cm)	Length of the longest stolon, typically the primary shoot, from base (or soil surface) to apical bud.	Stem growth
# internodes on longest stolon	The youngest internode was included only when longer than 1 cm for the cultivars, and 0.5 cm for Finnmark plants.	Average internode length
# branches exceeding the pot	Branches of which at least 5 cm of the stem was exceeding the pot rim.	Branching

2.5.2 Stomatal Characteristics

Stomatal characteristics were examined to assess whether leaf surface anatomy could contribute to differences in stomatal conductance. Epidermis imprints were used to determine stomatal density and length, on both adaxial and abaxial leaf surfaces. Three genotypes of each type, in both treatments, were included in this analysis, conducted at the end of Experiment 1. Imprints of both leaf surfaces were made on one mature, healthy leaf from each plant. Nail polish (All Clear, H&M Hennes & Mauritz GBC AB, Stockholm, Sweden) was applied in a thin layer, on the abaxial surface of one leaf piece and on the adaxial side of another,, and left to dry for a few minutes. A piece of clear tape was pressed onto the nail polish, the imprint was peeled off and taped onto a glass microscope slide.

Densities and lengths of stomata were determined by microscopic examination of the imprints. For the abaxial imprints, an Axioplan2 imaging microscope (Carl Zeiss AG, Oberkochen, Germany) equipped with an Axio cam HDR camera (Carl Zeiss AG, Oberkochen, Germany) was used. As the cells were smaller in the adaxial imprints (Fig.

9), higher magnification was needed. Transmission images were acquired on an Olympus IX 83 microscope, equipped with two Hamamatsu ORCA-flash 4.0 cameras and a 30X 1.05NA (UPLSAPO30XSIR) silicon immersion objective. The microscope was controlled by the CellSens software (Olympus Life Sciences Solutions, Waltham, MA, USA). Stomata were counted in a 480 x 350 µm area for the abaxial imprints, and 333 x 333 µm area for the adaxial, using the forbidden line method. The sizes of three random stomata were measured as the outer longitudinal length of the two guard cells (Fig. 9). The measurements were conducted using Fiji software.

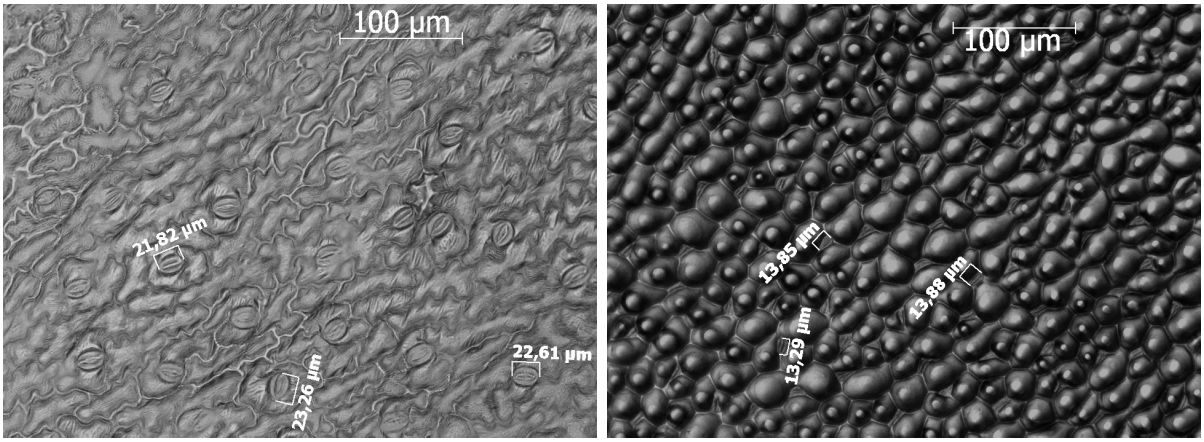

Figure 9: Example of an epidermis imprint of the abaxial (left) and adaxial (right) leaf surface of a Finnmark *Trifolium repens*, with length measurements of three random stomata. The light "dots" centered at the cell surfaces on the adaxial side are papilla, that were present on the adaxial side only in all analysed leaves (in line with Zoric et al., 2009).

2.6 Data Analysis

2.6.1 Data-preparation: Diurnal Measurements of Gas Exchange

The diurnal gas exchange measurements (section 2.3.2) resulted in 18 series of measurements logged every 60 – 90 s for approximately 24 – 26 h. Calculations of stomatal conductance (g_s) and net photosynthetic rate (A_n) from raw data were done as given by the LI6400 software, which is based on established gas exchange theory (LI-COR Biosciences, 2012). As the measurements generally needed some time to stabilise, the first 30 – 60 measurements were removed. At what time a series was cut was determined through visual inspection of plots of time against stomatal conductance, photosynthesis, temperature, relative humidity and CO_2 concentration. For one of the Litago genotypes in LL, the relative humidity was very high (>90%) about 21:00

– 03:00, in both the reference and leaf chamber. This resulted in unreliable measurements that were excluded. Also, for one Finnmark and one Milkanova genotype in HL, approximately 1.5 h and 1 h respectively, of the A_n measuring series during the night were removed. This was due to abrupt changes in A_n caused by CO_2 regulation errors. The removed intervals occurred within otherwise stable day/night levels, for which only averages are used for statistical analysis. The analysed values are therefore probably not affected by the removed intervals.

Calculation of g_s for the diurnal measurements includes the stomatal ratio, defined as the fraction of stomatal conductance of one side of the leaf to the other (LI-COR Biosciences, 2012). Stomatal ratios were calculated from the point measurements of stomatal conductance, done in Experiment 1 (Section 2.3.1), where both sides were measured. For each *T. repens* type, the average stomatal ratio for both light treatments in the time intervals 08:30 – 09:00 and 11:30 – 13:00 were used. Stomatal ratios within the types were similar in the two light treatments.

For plotting g_s and for calculating the adjusted A_n (see below), moving averages were used. Moving averages with periods of ten were calculated using the five values before and four after each time point. This was done to reduce mechanically caused noise (as these short-term fluctuations were also present in the reference chamber, it was caused by instrument regulation and not real physiological changes in the leaf). For series exceeding 24 h, averages were used for the time of the day where the first and last measurements overlapped (for example, if a series started at 12:00 and ended at 13:00 the next day, averages of the first and second day were used for the interval 12:00 – 13:00).

As noted in Section 2.2.2, the light intensity during the day was different in the two light treatments during Experiment 2. This is an unfortunate source of error, in particular when considering photosynthetic rate. As A_n is (approximately) linearly related to light intensity, up to the light-saturation point, a direct comparison of A_n between the two light treatments would only reflect the difference in light intensity (Ehleringer & Sandquist, 2018, p. 250). To compare the results (although probably still influenced by the difference in light intensity), A_n was adjusted by dividing by PPFD in the leaf chamber (PARi). For each time point, moving averages with periods of ten for

A_n and PARi were used. This adjustment of A_n is based on the assumption that the measurements are in the linear area of the light response curves for these leaves. This seems reasonable based on light response curves of Finnmark *T. repens* (Fig. A.6), and that light saturation occurs between 500 –1000 µmol/m^{2}s for most leaves (Ehleringer & Sandquist, 2018, p. 251). The highest PARi values in the diurnal measurements were around 240 µmol/m^{2}s. Moreover, higher light intensities in the growth environment generally elevate the light-saturation point (Ehleringer & Sandquist, 2018, p. 251), possibly extending the linear area of the light response curves for plants grown in higher light intensities. Stomatal conductance did not show any clear association with PARi at these light intensities, and was not adjusted. An adjusted water use efficiency was calculated as the adjusted A_n divided by g_s.

For statistical analysis of the diurnal gas exchange measurements, a series of aggregated values were calculated and compared (Table 3). For these calculations, the time point for when the white light was turned on was defined as the last measurement before a PARi greater than 10 µmol/m^{2}s was measured. This time point varied from 08:55 to 09:55, but was defined as 09:00 in all measuring series to make time points directly comparable. Mean day values of g_s and adjusted A_n were calculated from measurements between 10:45 – 02:45 and 10:00 – 02:45, respectively. This was done in order to compare the day levels after stabilisation in the morning. Measurements between 03:30 and 08:30 were used to calculate mean night g_s and respiration, thus only including the period with darkness in LL (Fig. 3). The time points at which g_s had reached its maximum in the morning, and A_n its day-level, were determined by visual inspection of the measurements plotted against time. The time point at which light was turned off was defined as the last measurement before a PARi less than 10 µmol/m^{2}s was measured. The time point at which g_s had reached its night level was defined as the first measurement after light was turned off for which the differences from the measurement before and after were less than 0.0010 mol H_2O/m^{2}s. The calculations were conducted in RStudio with R version 4.1.1 (R Core Team, 2021).

2.6.2 Statistical Analysis

This section provides an overview of the models used for data analysis. Analyses of variance (ANOVA) were conducted for most of the measured variables. Depending on

whether clones were included as replicates for each genotype, one of two linear models were used for each ANOVA: *Model 1* or *Model 2*. The analyses were conducted in RStudio with R version 4.1.1 (R Core Team, 2021), using the package *mixlm* (Liland, 2021) for ANOVAs. Method of moments was used for estimating variance parameters. The significance level was set to 5% for all analyses.

Model 1

For some of the analyses, clones of each genotype were included as replicates (Fig. 10).

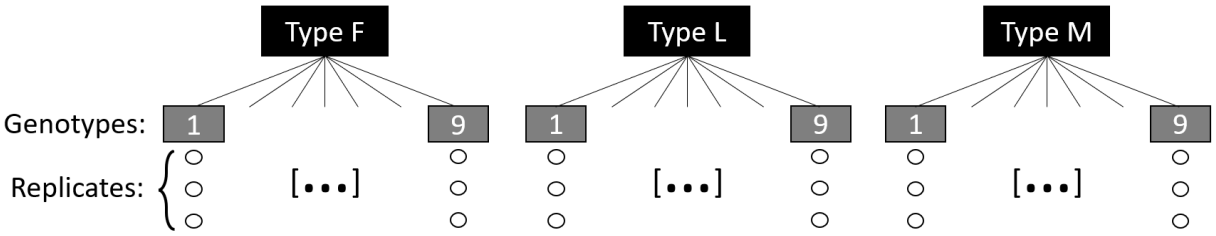

Figure 10: Illustration of the nested design, where *genotype* is nested under *type* (F = Finnmark, L = Litago, M = Milkanova). Three clones of each genotype constitute the replicates. This design is repeated in the two light treatments.

This resulted in a nested factorial design, and the effects model applied on these situations will be referred to as *Model 1* (model components are explained in Table 2):

$$y_{ijkt} = \mu + \tau_i + \beta_j + g_{k(j)} + (\tau\beta)_{ij} + (\tau g)_{ik(j)} + e_{(ijk)t} \tag{1}$$

where

$$\sum_{i=1}^{2} \tau_i = \sum_{j=1}^{3} \beta_j = 0$$

$$\sum_{i=1}^{2} (\tau\beta)_{ij} = 0 \quad , \forall j$$

$$\sum_{j=1}^{3} (\tau\beta)_{ij} = 0 \quad , \forall i$$

$$g_{k(j)} \overset{iid}{\sim} N(0, \sigma_g^2), \;\; (\tau g)_{ik(j)} \overset{iid}{\sim} N(0, \sigma_{\tau g}^2), \;\; e_{(ijk)t} \overset{iid}{\sim} N(0, \sigma^2)$$

and $i = 1, 2$ (HL and LL), $j = 1, 2, 3$ (Finnmark, Litago, Milkanova), $k = 1, \cdots, 9$ (genotypes of each type), and $t = 1, 2, 3$ (clones of each genotype).[4] Greek letters

[4] iid = independently and identically distributed

indicate fixed effects and parameters, while Latin letters indicate random effects and variables (Table 2). *Light treatment* and *type* are considered fixed effects, while *genotype* is considered a random effect nested under *type*. Starting with the full model, backward selection was performed using p-value ≤ 0.05 as selection criteria.

Table 2: Description of the components of Model (1)

Parameter/variable	**Description**
y_{ijkt}	Observed value for clone (replicate) t of genotype k of clovertype j, in light treatment i. The response variables are listed in Table 3
μ	Overall expected value
τ_i	Parameter describing the main effect (deviation from μ) of light treatment i
β_j	Parameter describing the main effect of type j
$g_{k(j)}$	Random variable describing the effect of genotype k, nested under type j
$(\tau\beta)_{ij}$	Parameter describing the interaction between light treatment and type
$(\tau g)_{ik(j)}$	Random variable describing the interaction between light treatment and genotype within type j
$e_{(ijk)t}$	Error term. Random variable describing the deviation of y_{ijkt} from the expected value for genotype k of type j, in light treatment i
σ^2	Parameter describing the variance of the error terms
σ^2_g	Parameter describing the variance of genotypes within the types
$\sigma^2_{\tau g}$	Parameter describing the variance of the interaction between light treatment and genotype within type

Model 2

When only one clone of each genotype was included, the genotypes are regarded as replicates of each type (Fig. 11).

Figure 11: Illustration of the completely randomised design, where genotype is regarded as replicates of each type. In this setting, the response is the difference in the variable of interest between a pair of clones of the same genotype in the two light treatments. Therefore, it is analysed as a single factor ANOVA with *type* as the only factor.

This results in a completely randomised design, and the effects model applied on these situations will be referred to as *Model 2*:

$$y_{jk} = \mu + \beta_j + e_{jk} \tag{2}$$

where

$$\sum_{j=1}^{3} \beta_j = 0$$

and

$$e_{jk} \overset{iid}{\sim} N(0, \sigma^2).$$

Here, the response, y_{jk}, is the difference of the measured variable between a pair of clones of the same genotype in the two light treatments (HL - LL), and μ is the overall expected value of this difference. The interpretation of β_j and the error term thus changes slightly: β_j is now the effect of *type* on the difference between the two light treatments - analogous to the interaction term $(\tau\beta)_{ij}$ in Model 1. The error term, e_{jk}, describes the deviation of y_{jk} from the expected value for type j. The overall mean difference (μ), represents the effect of the light treatment in this model. An overview of when each of the two models are used is given in Table 3.

Tukey's tests were performed when interaction between the effect of light treatment and type was significant. That is, for $(\tau\beta)_{ij}$ in Model 1 and β_j in Model 2.

Table 3: Overview of response variables analysed in ANOVAs. In Model 1, the clones (C) are the replicates, and genotype is considered a random factor with number of levels given in this table (G). For model 2, genotypes (G) are considered replicates and only one clone is included per genotype in each treatment. For petiole length, and leaflet vein length the replicates are averages of three repeated measurements (Table 1). Diff. = Differences in the measured value between pairs of the same genotype in the two light treatments (HL - LL), g_s = stomatal conductance, A_n = photosynthetic rate, adjusted A_n = A_n divided by light intensity, N/C = leaf blade nitrogen to carbon ratio, SLA = specific leaf area, ada. = adaxial, aba = abaxial, sum = sum of variable for both surfaces.

Experiment	Measurement	Model	Response variable	G	C
Experiment1	Chlorophyll content	(1)	Chlorophyll content per leaf area ($\mu g\ chl.\ a/cm^2$)	9	3
	Leaflet vein length (proxy for leaflet area)		Squared leaflet vein length (cm^2)	9	3
	Petiole length		Petiole length (cm)	9	3
	Length of longest stolon		Length of longest stolon (cm)	9	3
	Length/#internodes for the longest stolon		Average internode length (cm)	9	3
	#Branches exceeding the pot		#Branches exceeding the pot	9	3
	Length of stomata		Length of stomata (μm)	3	3*
	Stomatal density (ada., aba., sum)	(2)	Diff. Stomatal density ($\#stomata/mm^2$) (ada., aba., sum)	3	
	Point measurements of g_s		Diff. g_s sum in each time interval	9	
	Leaf blade N and C content		Diff. N/C	3	
	Leaf blade area and dry weight		Diff. SLA (cm^2/mg)	3	
Experiment2	Diurnal measurements of gas exchange	(2)	Diff. average night g_s	3	
			Diff. average day g_s		
			Diff. time from light is turned on to max. g_s		
			Diff. max. g_s		
			Diff. (average day g_s/max g_s)		
			Diff. time from light is turned off to night level g_s		
			Diff. average adjusted A_n		
			Diff. time from light is turned on to max. A_n		
			Diff. average adjusted WUE		
			Diff. average night respiration		

*For stomata lengths, three randomly chosen stomata on the same leaflet are considered replicates of a genotype.

Model adequacy checking

The ANOVA assumptions of normally distributed error terms and equal variance were tested visually using quantile-quantile plots and plots of fitted values against residuals, respectively. These plots are shown in the Appendix (A.6).

Linear regression

As a preliminary analysis of the point measurements, the time dependency of stomatal conductance in each time interval was assessed visually. No correlation with time was found in the intervals 08:30 – 09:00, 11:30 – 13:00, or 16:00 – 17:00. However, in the interval 09:00 - 10:00, g_s tended to increase with time (later confirmed by the diurnal measurements), as expected. g_s in the interval 09:00 - 10:00 was therefore considered a function of time. The diurnal measurements of g_s showed that after an initial increase, g_s generally started to sink again around 09:45 - 10:00. Point measurements in the 09:00 - 10:00 interval conducted after 09:45 was therefore excluded, to restrict the interval to the linear area as far as possible. This resulted in exclusion of four observations, one of each of the following: Litago and Milkanova in HL, Milkanova and Finnmark in LL. The interval is from now on referred to as 09:00 – 09:45. Regression coefficients were estimated through least squares regression for each type in both light treatments. 95% confidence intervals were calculated for the regression coefficients and used for comparison, together with R^2-values.

3 Results

3.1 Gas Exchange

3.1.1 Point Measurements of Stomatal Conductance

Stomatal conductance (g_s) was generally higher in the high latitude light treatment (HL) in the time intervals 08:30 – 09:00, 11:30 – 13:00, and 16:00 – 17:00 (Fig. 12 and 13). Due to a pronounced difference in the variance between the time-intervals (Fig. 13), a separate ANOVA was conducted for each. The difference between light treatments was significant only for the 11:30 – 13:00 interval (Table 4). However, mean g_s for the two cultivars (Litago and Milkanova) were higher in HL for the two other intervals as well. The three *T. repens* types did not differ significantly in their responses to light treatment in any of the intervals. However, Finnmark consistently had the lowest estimate for the difference HL - LL (mean g_s was even lower in HL in two of the intervals) (Table 4). This indicates an increased g_s in HL for the cultivars (the largest response was that of Milkanova 11:30 – 13:00) that was not evident for Finnmark, although the difference was not significant.

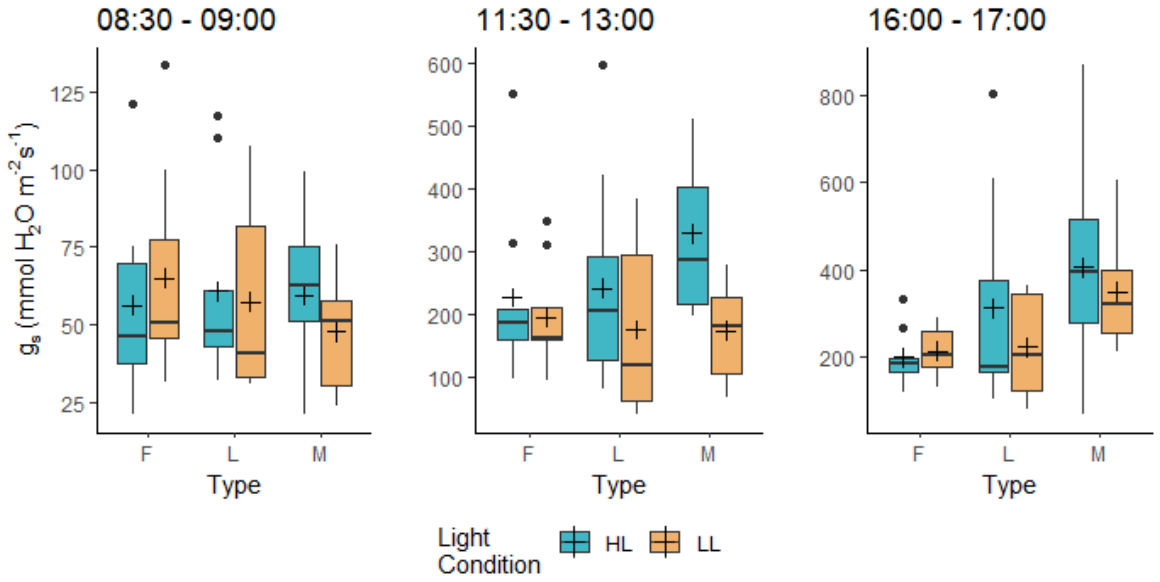

Figure 12: Point measurements of stomatal conductance in three time intervals (Experiment 1), results in absolute values. Note the different scales. The observations are sums of both leaflet sides, for one clone per genotype (nine replicates) for each type (F = Finnmark, L = Litago, M = Milkanova) in both light treatments (HL = High latitude, LL = Low latitude). During the interval 08:30 – 09:00, low-intensity blue light was on in both treatments, while white growing light was on in the two other intervals. Boxes show the first and third quartiles, with the median indicated by a line, and whiskers extending to the largest and smallest value within 1.5*inter-quartile range (points outside this are plotted individually). Crosses show mean values.

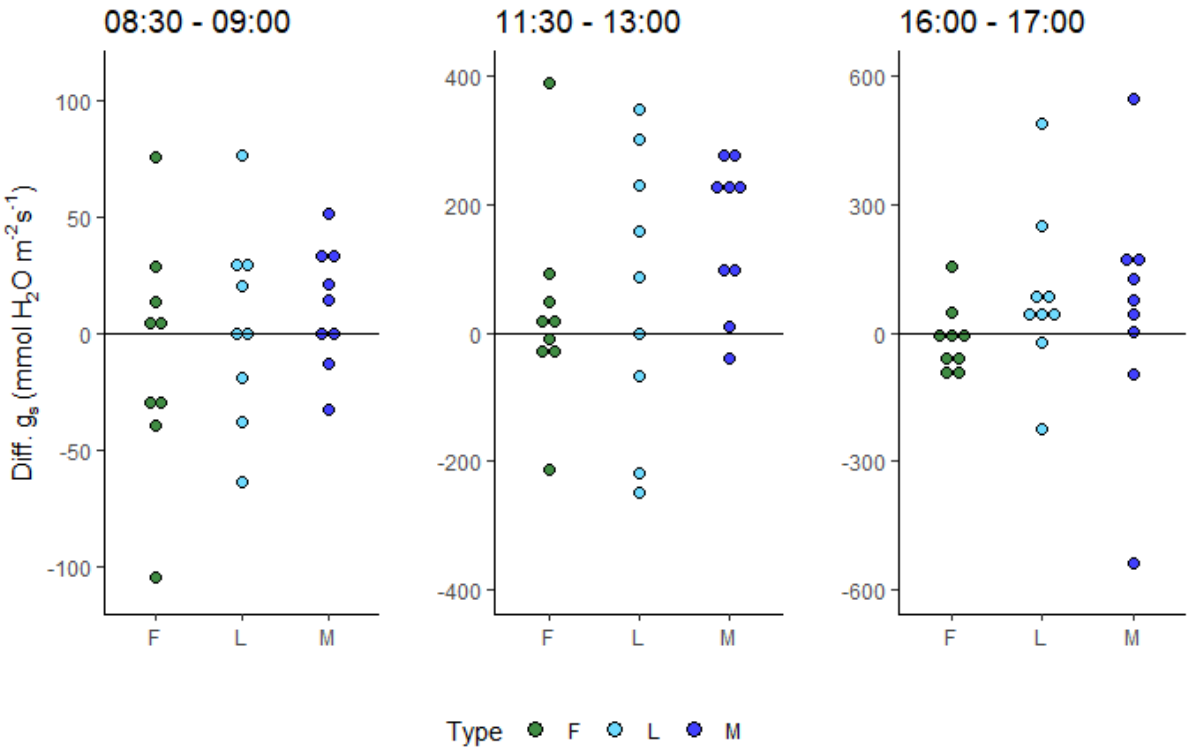

Figure 13: Point measurements of stomatal conductance (g_s) in three time intervals for each type (F = Finnmark, L = Litago, M = Milkanova). Each point is the difference (High latitude - Low latitude) in stomatal conductance (sum of both leaflet sides) between a pair of clones of the same genotype in the two light treatments. Nine genotypes (replicates) are included per type. Note the different scales.

Table 4: Analyses of variance for point measurements of stomatal conductance, using Model 2. The response variable is the pairwise differences between the two light treatments (HL - LL, Fig 13). Lt = overall mean difference (represents the effect of light treatment), T = type (the effect of type on the difference between the two light treatments). $\hat{\beta}$ describes the estimated effect (deviation from the overall mean, μ) of each type (F = Finnmark, L = Litago, M = Milkanova).

Time interval	Source	Estimates	F-value	p-value
08:30 – 09:00	Lt	$\hat{\mu}$ = 2.10	0.0725	0.790
	T	$\hat{\beta}_F$= -10.9, $\hat{\beta}_L$= 1.44, $\hat{\beta}_M$= 9.49	0.577	0.570
11:30 – 13:00	Lt	$\hat{\mu}$ = 84.5	6.76	**0.016**
	T	$\hat{\beta}_F$= -52.4, $\hat{\beta}_L$= -18.6, $\hat{\beta}_M$= 71.0	1.28	0.296
16:00 – 17:00	Lt	$\hat{\mu}$ = 44.0	1.24	0.276
	T	$\hat{\beta}_F$= -57.8, $\hat{\beta}_L$= 45.2, $\hat{\beta}_M$= 12.6	0.592	0.561

Point measurements of g_s in the interval 09:00 - 09:45 were analysed as linear functions of time (Fig. 14). There was considerable variation within types, and 95% confidence intervals for the regression coefficients overlapped substantially (Table A.6), indicating that there is considerable variation within types in this interval, which should be kept in mind when considering the diurnal measurements of stomatal conductance.

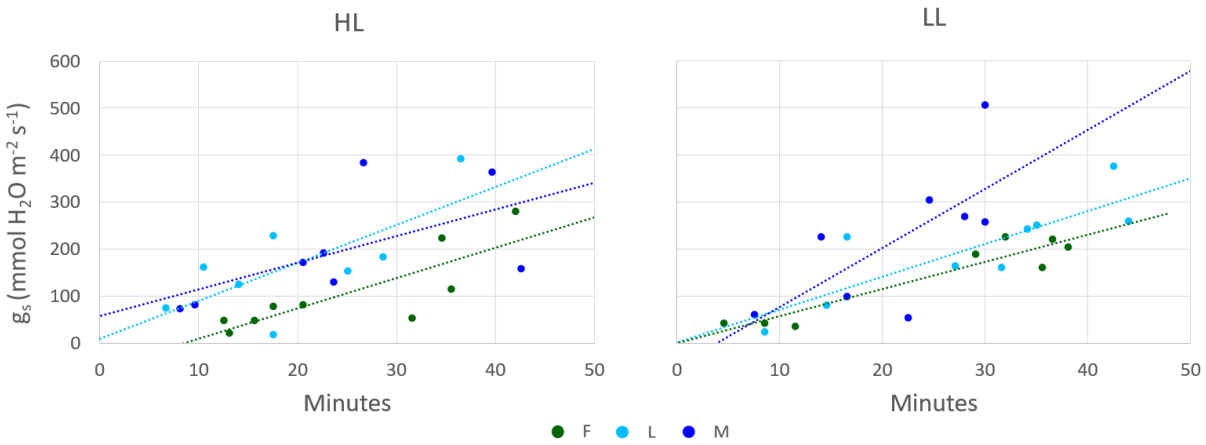

Figure 14: Point measurements of stomatal conductance (g_s, mol H_2O $m^{-2}s^{-1}$) as a function of time the first 45 min after white light was turned on (at 09:00). Least squares regression lines are shown for each type (F = Finnmark, L = Litago, M = Milkanova) in two light treatments (HL = High latitude, LL = Low latitude). The observations are the sums of both sides of a leaflet, with one observation per genotype.

3.1.2 Diurnal Measurements of Stomatal Conductance and Photosynthesis

No significant effect of light treatment was found for any of the analysed variables in the diurnal gas exchange measurements. Due to the low number of replicates, and the error in light intensity during the day (Section 2.2.2), these results should be handled with care. The observed main patterns are presented here.

Stomatal conductance

The diurnal measurements of stomatal conductance did not show any significant difference between light treatments in the mean stomatal conductance during the day, nor at night (Fig. 15; Table 5). In general, each measuring series fluctuated around a "day-level" g_s when the white growing light was on, and a low "night-level" when the white light was off, except from a pronounced peak during the first 1 - 1.5 h with white light in the morning. For some of the curves, there seems to be a slight increase in g_s during the second half of the photoperiod. However, this could be an effect of at what time the measurements were started (mainly between 14:00 and 22:00). The responses of the three types in mean g_s did not differ significantly, neither during the day nor at night. However, the Litago genotypes tended to have higher day g_s in HL. One of the Milkanova genotypes in HL show notably low g_s values. Problems with the temperature sensors during this measurement, may have resulted in artificially low g_s values.

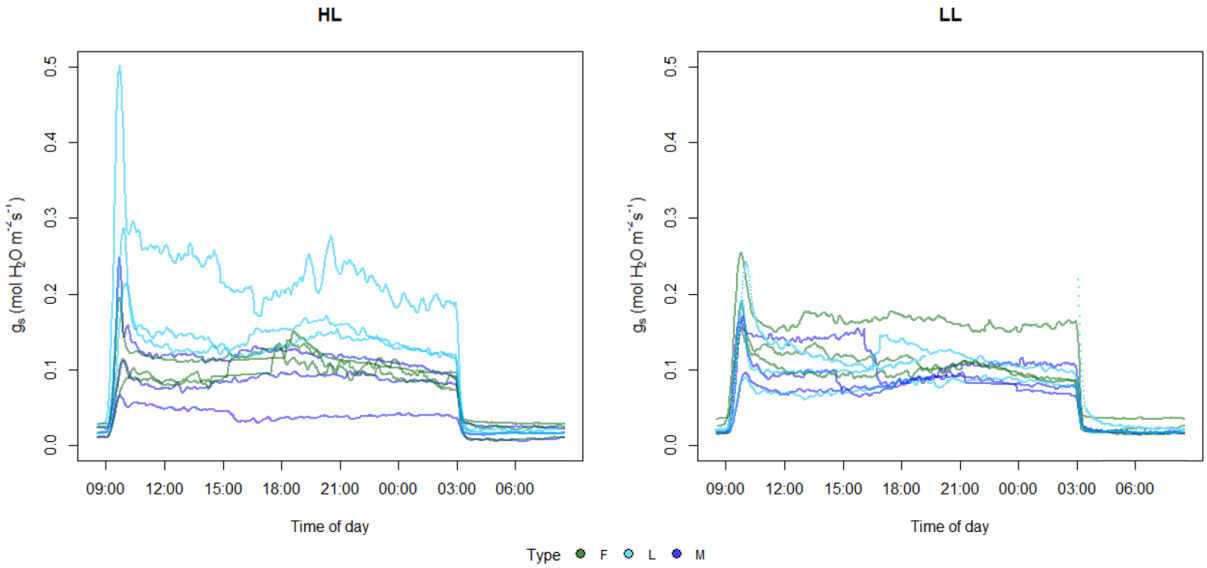

Figure 15: Diurnal measurements of stomatal conductance (g_s, mol H_2O $m^{-2}s^{-1}$) conducted during Experiment 2 for each type (F = Finnmark, L = Litago, M = Milkanova) in two light treatments (HL = High latitude, LL = Low latitude). Moving averages with periods of ten are shown. White growing light was turned on in both rooms at 09:00, and off at 03:00. Low-intensity blue light was on 08:30 – 09:00 and 03:00 - 03:30 in LL, while it was on all night in HL. Three genotypes per type were included, with one clone in each light treatment. Some curves have an abrupt change in g_s level during the day (most pronounced for two of the Milkanova genotypes in LL) caused by the onset/end of the measurement. All measuring series were started at different time points, but all during the photoperiod.

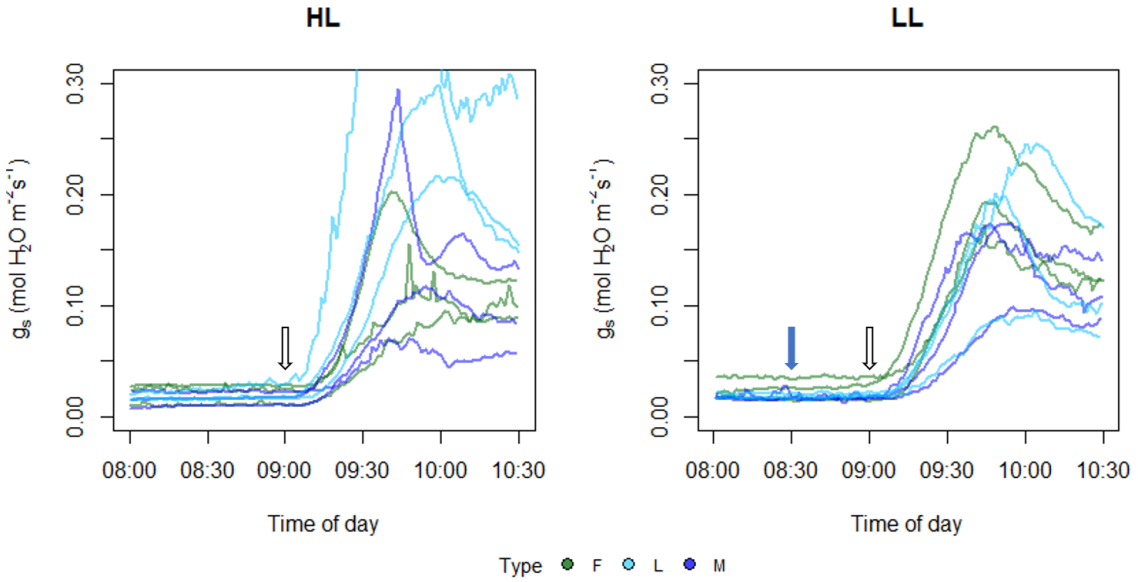

Figure 16: Details of the plots shown in Fig. 15: Stomatal conductance when light is turned on in the morning, in the two light treatments (HL = High latitude, LL = Low latitude). White arrows indicate when the white light is turned on, while the blue arrow shows when the low-intensity blue light is turned on in LL. In HL, the weak blue light is on the entire night. The highest peak in HL is at approximately 0.5 mol H_2O m^{-2} s^{-1}, and is outside the figure range.

No response in g_s was observed when the weak blue light was turned on in LL (Fig. 16). However, after a lag phase of about 5 – 15 min, a strong response was observed in both treatments when the white light was turned on. This pronounced increase in g_s culminated in a peak before sinking to a day-level, although there was considerable variation in the magnitude of the peak. No significant difference between the treatments was found for neither the maximum g_s reached in the peak nor for the time required to reach it (Table 5). The three types did not respond significantly different to light treatment with respect to the height or time point of the peak. However, Finnmark consistently diverged from the two cultivars in the estimated response (Table 5). And the difference HL – LL in $Mean\ day\ g_s/Max\ g_s$ significantly differed between Finnmark and Litago, and tended to differ between Finnmark and Milkanova ($p = 0.056$).

Photosynthesis

Photosynthetic assimilation rate (A_n) was higher in HL due to the higher light intensity (Fig. 17; Section 2.2.2). However, when A_n was adjusted for light intensity, no effect of light treatment was evident (Fig. 18; Table 5). When white light was turned on in the morning, there was generally an initial rapid increase in photosynthesis, followed by a slightly slower increase until a plateau was reached. After reaching the plateau, A_n fluctuated around a relatively stable day-level until the light was switched off. The adjusted values of these day-levels are shown in Figure 18. The non-adjusted A_n

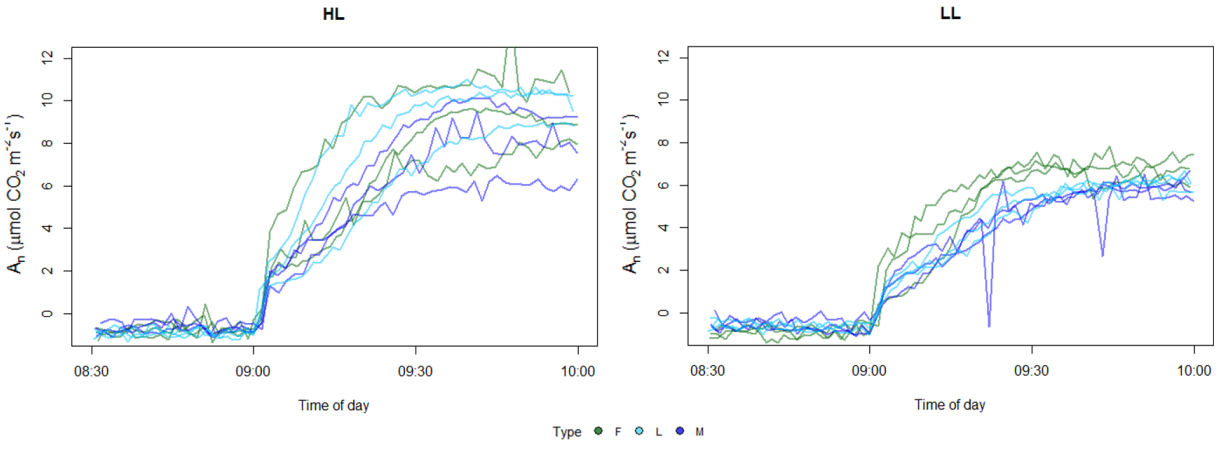

Figure 17: Photosynthetic assimilation rate (A_n, non-adjusted, µmol CO_2 m^{-2} s^{-1}). The short-time fluctuations are partly caused by variation in the CO_2 regulation in the reference- and leaf chamber. White growing light was turned on in both rooms at 09:00. Low-intensity blue light was turned on 08:30 in LL, while it was on all night for HL.

values were only used to determine the time required to reach the day-level plateau, for which no significant effects could be shown (Table 5). For all replicates in both treatments, the A_n plateau was reached before the peak in g_s (Fig. 17 and 16). Concerning night respiration, no overall effect of light treatment was found, but Litago diverged from the other types (significantly from Milkanova) with higher night respiration in HL (Table 5; Fig. A.12).

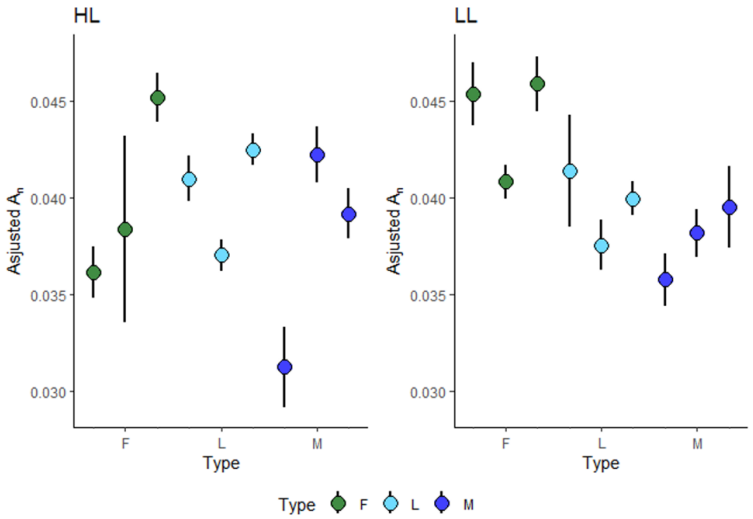

Figure 18: Day-level net photosynthetic assimilation rate (A_n) adjusted for the non-intended difference in light intensity between the two light treatments (HL = High latitude, LL = Low latitude). Dots and lines show means ± 1 standard deviation (µmol CO_2 / µmol photones). Clones of the same genotypes are shown in the same order for both light treatments.

Table 5: Results of AVOVAs for the aggregated values from diurnal measurements of gas exchange, using Model 2 (with pairwise differences of each value between clones of the same genotypes in the two treatments as response). Lt = overall mean difference (represents the effect of light treatment), T = type (the effect of type on the difference between the two light treatments). $\hat{\beta}$ describes the estimated effect (deviation from the overall mean, μ) of each type (F = Finnmark, L = Litago, M = Milkanova). Night respiration is given in terms of negative CO_2 uptake.

Value	Source	Estimates			F-value	p-value	Tukey p-values
Mean night g_s	Lt	$\hat{\mu}$ = -0.00245			0.665	0.446	
	T	$\hat{\beta}_F$= -0.00104,	$\hat{\beta}_L$= 0.000149,	$\hat{\beta}_M$= 0.000889	0.0348	0.966	
Mean day g_s	Lt	$\hat{\mu}$ = 0.0108			0.459	0.523	
	T	$\hat{\beta}_F$= -0.0307,	$\hat{\beta}_L$= 0.0527,	$\hat{\beta}_M$= -0.0220	2.76	0.141	
g_s increase time	Lt	$\hat{\mu}$ = -0.293			0.0108	0.921	
	T	$\hat{\beta}_F$= 8.41,	$\hat{\beta}_L$= -4.25,	$\hat{\beta}_M$= -4.17	2.24	0.188	
Max g_s	Lt	$\hat{\mu}$ = 0.0373			0.930	0.372	
	T	$\hat{\beta}_F$= -0.105,	$\hat{\beta}_L$= 0.129,	$\hat{\beta}_M$= -0.0243	3.14	0.116	
Mean day g_s/Max g_s	Lt	$\hat{\mu}$ = 0.00486			0.0153	0.905	
	T	$\hat{\beta}_F$= 0.203,	$\hat{\beta}_L$= -0.120,	$\hat{\beta}_M$= -0.0824	6.77	**0.029**	L-F: **0.035**, M-F: 0.056, M-L: 0.919
g_s decrease time	Lt	$\hat{\mu}$ = -0.119			0.00190	0.967	
	T	$\hat{\beta}_F$= 3.24,	$\hat{\beta}_L$= -1.13,	$\hat{\beta}_M$= -2.11	0.364	0.709	
Mean adjusted A_n	Lt	$\hat{\mu}$ = -0.00128			1.06	0.344	
	T	$\hat{\beta}_F$= -0.00285,	$\hat{\beta}_L$= 0.00182,	$\hat{\beta}_M$= -0.00103	1.34	0.330	
A_n increase time	Lt	$\hat{\mu}$ = 1.58			0.736	0.424	
	T	$\hat{\beta}_F$= 2.34,	$\hat{\beta}_L$= 0.422,	$\hat{\beta}_M$= -2.77	0.652	0.554	
Mean adjusted WUE	Lt	$\hat{\mu}$ = -0.00757			0.0125	0.915	
	T	$\hat{\beta}_F$= 0.0222,	$\hat{\beta}_L$= -0.133,	$\hat{\beta}_M$= 0.111	1.11	0.388	
Mean night respiration	Lt	$\hat{\mu}$ = -0.0899			2.69	0.152	
	T	$\hat{\beta}_F$= 0.0870,	$\hat{\beta}_L$= -0.280,	$\hat{\beta}_M$= 0.193	6.82	**0.029**	L-F: 0.076, M-F: 0.723, M-L: **0.029**

3.2 Leaf Blade Composition

3.2.1 Chlorophyll Content

No difference in chlorophyll content was found between the light treatments, nor between the types (Fig. 19; Table A.7). The differences between genotypes contributed significantly to the observed variation (Table A.7).

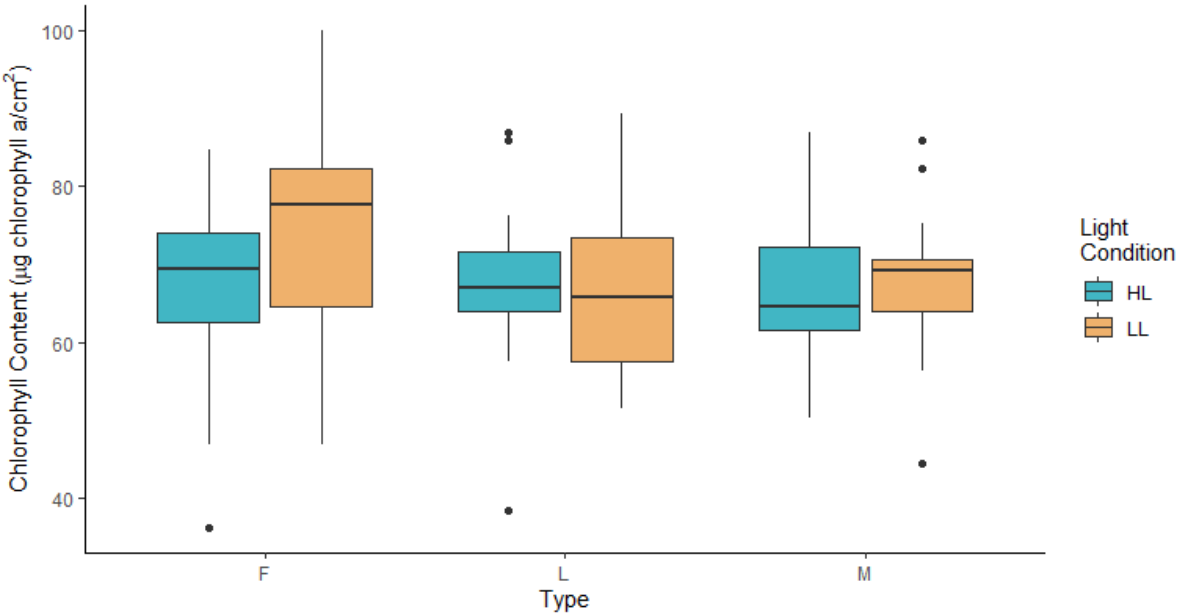

Figure 19: Chlorophyll content in the two light treatments (HL = High latitude, LL = Low latitude) measured with a chlorophyll content meter and converted to absolute values (µg chlorophyll a/cm^2), using a standard curve constructed for *T. repens* (Fig. 8). Three clones of each of nine genotypes were included per type (F = Finnmark, L = Litago, M = Milkanova), except for F in HL of which one clone was missing. Boxes show the first and third quartiles, with the median indicated by a line, and whiskers extending to the largest and smallest value within 1.5*inter-quartile range (points outside this are plotted individually).

3.2.2 Leaf Blade Stochiometry and SLA

Specific leaf area (SLA) and the ratio of nitrogen to carbon content (N/C) in leaf blades were on average lower in the high latitude light treatment (Fig. 20), but no significant effect was found (Table 6). No difference between types was evident, however the variation within Milkanova was notably higher than for Litago and Finnmark. One of the Milkanova genotypes stood out by having higher values in HL for both N/C and SLA.

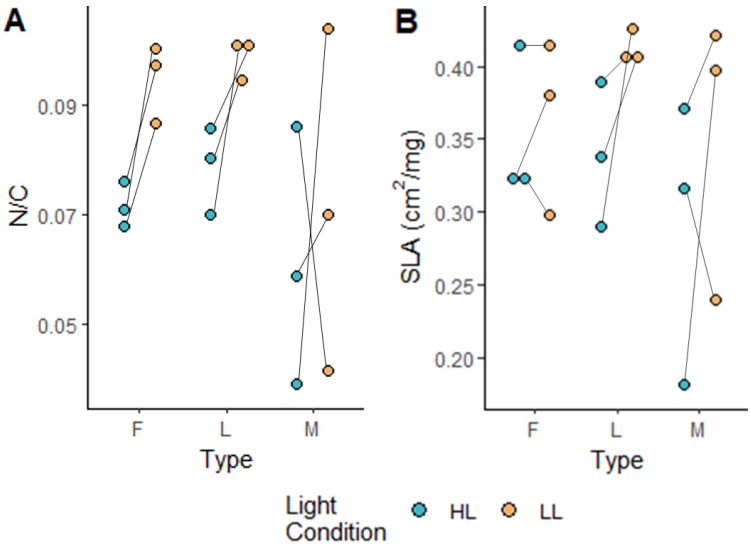

Figure 20: Pairwise differences in **A**) the ratio of nitrogen to carbon content (N/C) and **B**) specific leaf area (area/dry weight) of leaf blades. The black lines connect pairs of the same genotype in the two light treatments (HL = High latitude, LL = Low latitude). Three genotypes (replicates) were included per type (F = Finnmark, L = Litago, M = Milkanova).

Table 6: Results of ANOVAs for the ratio of nitrogen to carbon content (N/C) and specific leaf area (area/dry weight) of leaf blades, using Model 2. The response variable is the pairwise differences between the two light treatments (HL - LL, Fig. 20). Lt = overall mean difference (represents the effect of light treatment), T = type (the effect of type on the difference between the two light treatments). $\hat{\beta}$ describes the estimated effect (deviation from the overall mean, μ) of each type (F = Finnmark, L = Litago, M = Milkanova).

Response variable	Source	Estimates	F-value	p-value
Diff. N/C	Lt	$\hat{\mu}$ = -0.018	2.79	0.146
	T	$\hat{\beta}_F$= -0.005, $\hat{\beta}_L$= -0.002, $\hat{\beta}_M$= 0.008	0.130	0.881
Diff. SLA	Lt	$\hat{\mu}$ = -0.049	2.46	0.168
	T	$\hat{\beta}_F$= 0.038, $\hat{\beta}_L$= -0.024, $\hat{\beta}_M$= -0.014	0.383	0.697

3.3 Morphology

3.3.1 Plant Growth and Architecture

All three types showed clear morphological responses to light treatment (Fig. 21). Leaflet size, petiole length, maximal stolon length, average internode length, and branching were all significantly affected by light treatment (Table 7). All had higher

values in HL, except for branching which was lower. Accordingly there was an increased elongation of plant organs in HL, accompanied by increased apical dominance. For leaflet size (and to some degree petiole length), there were signs of heteroscedasticity and heavy tails in the residuals (Fig. A.10). I do not consider this to be severe enough to invalidate the model, as the differences were pronounced and the sample is relatively large and balanced. Differences between the genotypes contributed considerably to the variance in all plant growth and architecture variables. The effect of genotype and/or the interaction between genotype and light treatment were significant in all cases (Table 7).

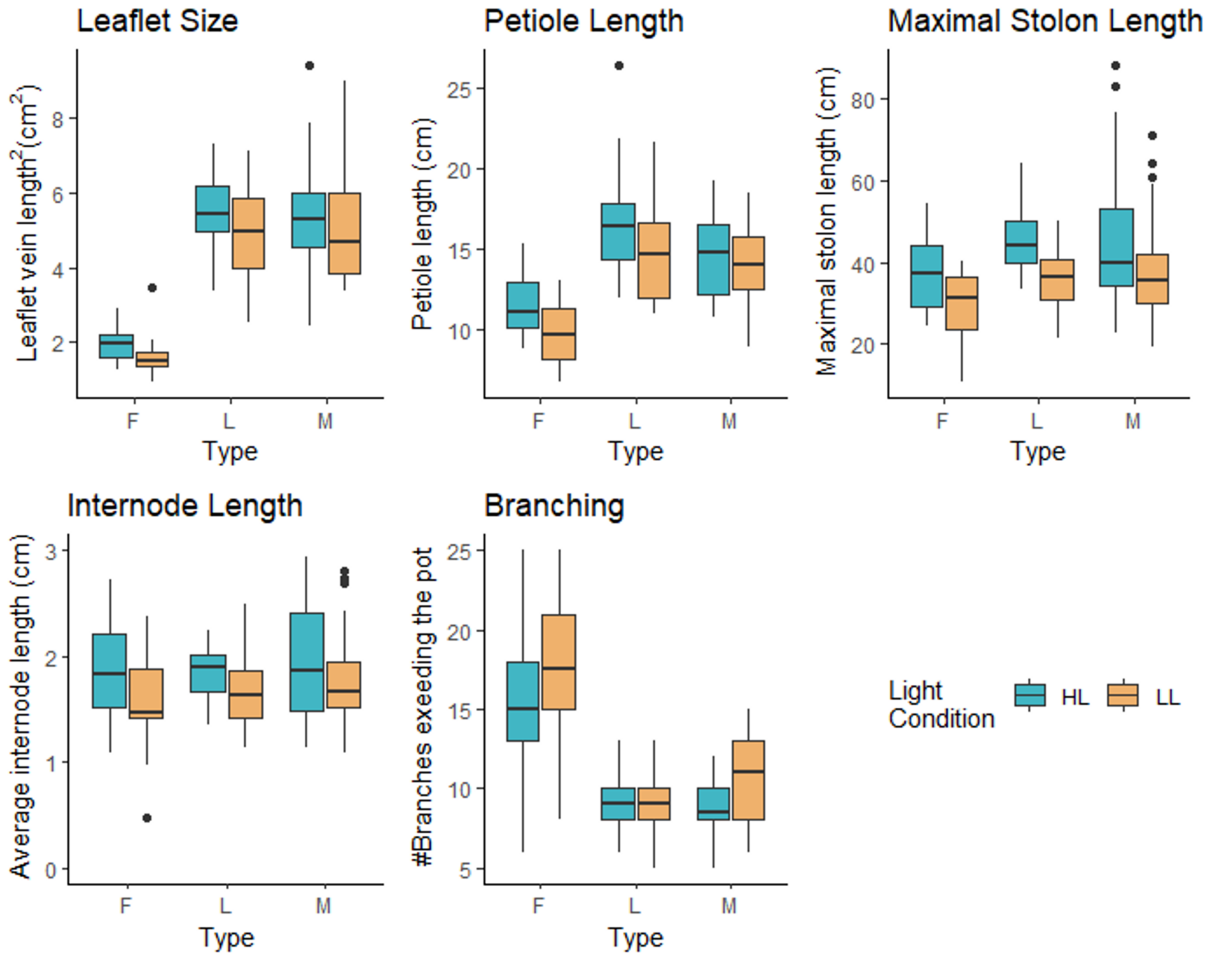

Figure 21: Effects of light treatment (HL = High latitude, LL = Low latitude) on plant growth and architecture in the three *T. repens* types (F = Finnmark, L = Litago, M = Milkanova). Three clones of each of nine genotypes were included per type, except for F in HL where one clone was missing. For leaflet size and petiole length, the observations were averages of three leaves per clone. Boxes show the first and third quartiles, with the median indicated by a line, and whiskers extending to the largest and smallest value within 1.5*inter-quartile range (points outside this are plotted individually).

The interaction term, Light treatment x Type (indicating differences between the types in their responses to light treatment) was only significant for branching (Table 7). The

Tukey's test showed that all three types differed significantly from one another: Adjusted p-values were <0.001 for Litago– Finnmark, 0.020 for Milkanova– Finnmark, and 0.026 for Milkanova– Litago. The mean response was largest for Finnmark, and negligible for Litago (estimates not shown). However, the types also differed significantly ($p < 0.001$) irrespective of the light treatments: The Finnmark plants were highly branched, while the cultivars clearly had fewer stolons per plant (Fig. 21).

Table 7: Results of ANOVAs for plant growth and architecture variables. Backwards selection was performed, starting with Model 1, with p-value ≤ 0.05 as selection criteria. The final model is given here. Lt = Light treatment, T = Type, G(T) = Genotype within Type.

Response	**Model**	**Source**	**F-value**	**p-value**
Leaflet size	$\mu + \tau_i + \beta_j + g_{k(j)} + e_{(ijk)t}$	Lt	10.4	**0.002**
		T	45.4	**<0.001**
		G(T)	7.26	**<0.001**
Petiole length	$\mu + \tau_i + \beta_j + g_{k(j)} + (\tau\beta)_{ij} + (\tau g)_{ik(j)} + e_{(ijk)t}$	Lt	8.76	**0.007**
		T	25.8	**<0.001**
		G(T)	1.49	0.166
		Lt x T	0.447	0.645
		Lt x G(T)	2.36	**0.002**
Maximal stolon length	$\mu + \tau_i + \beta_j + g_{k(j)} + (\tau\beta)_{ij} + (\tau g)_{ik(j)} + e_{(ijk)t}$	Lt	45.3	**<0.001**
		T	1.43	0.260
		G(T)	10.3	**<0.001**
		Lt x T	0.723	0.496
		Lt x G(T)	2.04	**0.007**
Average internode length	$\mu + \tau_i + \beta_j + g_{k(j)} + e_{(ijk)t}$	Lt	29.4	**<0.001**
		T	0.546	0.584
		G(T)	10.4	**<0.001**
Branching	$\mu + \tau_i + \beta_j + g_{k(j)} + (\tau\beta)_{ij} + e_{(ijk)t}$	Lt	22.0	**<0.001**
		T	24.6	**<0.001**
		G(T)	6.45	**<0.001**
		Lt x T	5.17	**0.007**

3.3.2 Stomatal Characteristics

No significant effects were found for stomatal densities (Table 8). It did however tend to be higher in HL for Milkanova, while the opposite tendency was observed for Finnmark (Fig. 22; Table 8). Stomatal densities were considerably higher on the adaxial sides compared to the abaxial (Fig. 22).

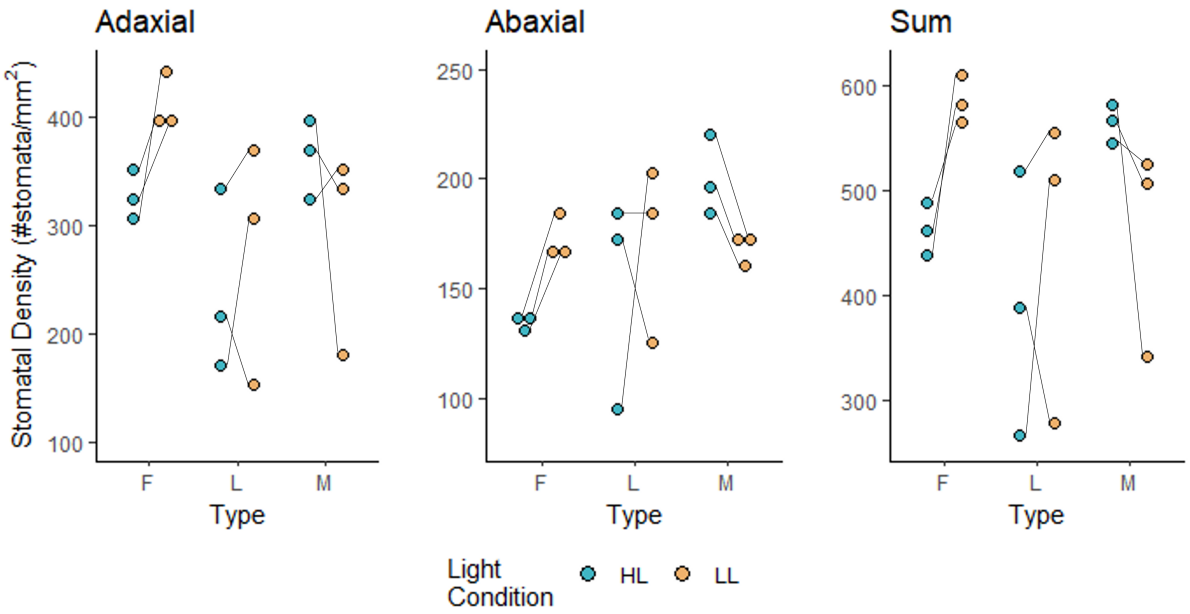

Figure 22: Stomatal densities. The points represent genotypes, which here constitute replicates each of the three types (F = Finnmark, L = Litago, M = Milkanova). The black lines connect pairs of the same genotype in the two light treatments (HL = High latitude, LL = Low latitude). Note the different scales.

Table 8: Results of ANOVAs for stomatal densities, for each leaf side and their sum, using Model 2. The response variable is the pairwise differences between the two light treatments (HL - LL, Fig. 22). Lt = overall mean difference (represents the effect of light treatment), T = type (the effect of type on the difference between the two light treatments). $\hat{\beta}$ describes the estimated effect (deviation from the overall mean, μ) of each type (F = Finnmark, L = Litago, M = Milkanova).

Leaf side	Source	Estimates	F-value	p-value
Adaxial	Lt	$\hat{\mu}$ = -15.1	0.218	0.657
	T	$\hat{\beta}_F$= -69.2, $\hat{\beta}_L$= -21.1, $\hat{\beta}_M$= 90.3	2.15	0.198
Abaxial	Lt	$\hat{\mu}$ = -8.60	0.305	0.601
	T	$\hat{\beta}_F$= -29.1, $\hat{\beta}_L$= -11.2, $\hat{\beta}_M$= 40.3	1.79	0.246
Sum	Lt	$\hat{\mu}$ = -23.7	0.317	0.594
	T	$\hat{\beta}_F$= -98.3, $\hat{\beta}_L$= -32.3, $\hat{\beta}_M$= 130	2.62	0.152

Light treatment did not seem to affect the length of stomata (Fig. A.13, Table A.8). The only significant effects were that of genotype within each type for the adaxial, and the interaction between light treatment and genotype (within type) for the abaxial stomatal lengths. As stomata on the same leaf were used as replicates of a genotype in this analysis, the differences between genotypes may also be attributed to differences between the sampled leaves. In all cases, stomata were considerably longer on the abaxial sides.

4 Discussion

Sources of Error and Limitations

Some potentially important sources of error and limitations, in addition to those pointed out in the Methods and Results sections, are considered here. The most severe source of error in this study was the unintended difference in day-time light intensity in the high latitude light treatment during Experiment 2 (Section 2.2.2). Despite the adjustment of A_n (Section 2.6.1), the difference in light intensity may have affected all the measured gas exchange variables, and the effect of light intensity cannot be distinguished from those of the intended light treatment. However, this error seems to have arisen after Experiment 1. It thus only affected the diurnal gas exchange measurements. I therefore consider the results from Experiment 1 more reliable.

In general, higher levels of stomatal conductance were measured with the porometer (point measurements) compared to the photosynthesis system (diurnal measurements). This could, at least partly, be explained by the lower relative humidity and higher temperature in the photosynthesis system leaf chamber (relative humidity was below 50% throughout the measurements for most replicates, while the room average was 68%). Lower relative humidity and higher temperatures increase vapor pressure deficit, which may have caused reduced stomatal opening. The air circulation in the leaf chamber may have enhanced this effect by reducing the leaf boundary layer. Such limitation to stomatal opening may have obscured the response to light treatment, but this effect could as well be negligible. The two instruments are based on different measuring technologies, and this may also have contributed to the different results. However, as the results from the two instruments were analyzed separately, this does not affect the point measurement results.

Additionally, there were recurring problems with temperature measurements in the photosynthesis system. Most measurements with this defect were re-taken. However, due to time-limitation and new technical problems, the least severe of these was included. This was a Milkanova replicate in HL, which had notably low g_s values and the lowest adjusted A_n values (Fig. 15 and 18). The faulty temperature measurements resulted in defective temperature regulation (as this is based on the measured

temperature in the instrument), and error in the calculation of stomatal conductance. As the real leaf chamber temperature was unknown, this could not be corrected for. The discrepancy between measured and real temperature could not be measured, as the magnitude of the error changed with the position of the sensor head. The faulty temperature measurements were higher than the real temperature (tested several times with an independent thermocouple). This has likely resulted in an underestimation of g_s for the one Milkanova replicate. However, the error seemed to have been constant throughout the measuring series, and the form of the curve is therefore valid.

The diurnal measurements only included three replicates per type, while the point measurements included nine replicates per type, which also makes them more reliable. The point measurements show a considerable variation between replicates (genotypes). As only one clone per genotype was included, the effect of genotype could not be distinguished from other sources of error. However, the high variation underpins the need for larger samples when studying gas exchange. For the diurnal measurements in this study, the sampled genotypes may thus have affected the results. A larger number of replicates was originally planned for the diurnal measurements but could not be completed due to delays caused by technical problems with the instrument and time-limitation.

During Experiment 1, the plants were infested by thrips and at the end of the experiment pathogenic fungi (resembling powdery mildew, order Erysiphales) were also evident. As this was the case in both light treatments and the plants were measured in a random order (within and between treatments), I assume it did not introduce bias in the analysis. Nevertheless, it did contribute to plant stress which may have affected the observed responses. Stomatal closure can be promoted by pathogen elicitors (Klüsener et al., 2002), hence fungi-infected leaves may have had reduced stomatal conductance. Infected and/or damaged leaves were avoided as far as possible during measurements. However, this only eliminated infection/damage visual for the naked eye. This was particularly challenging for the g_s point measurements during the 08:30 – 09:00 interval, as the weak blue "twilight" was the only light source. These problems gradually increased throughout the course of the experiment. This may have contributed to the observed variance in the point measurements of stomatal conductance, that were conducted over the course of several weeks. Avoiding damaged leaves also became

gradually more challenging, and for the leaf samples collected at the end of Experiment 1, some affected leaves had to be included. Only leaves older than at least third counting from apex were used but except from this, damage/infection was the main selection criteria. For the stomatal densities (where only three replicates were included), variation in leaf developmental stage may have affected the results if some of the leaves were not fully expanded.

4.1 Is Gas Exchange Through the Diurnal Cycle Affected by the Extended Twilight Period?

The results obtained in this thesis indicate that an extended twilight period increases the stomatal conductance during the day. A significant effect of light treatment on g_s, was found in the time interval 11:30 – 13:00 for the point measurements conducted in Experiment 1 (Table 4). The same tendency was also present in the intervals 08:30 – 09:00 and 16:00 – 17:00, with higher average g_s for the two cultivars (Litago and Milkanova) in HL (the effect of type on the response to light treatment could not be proven significant, this is further discussed in Section 4.3). Even though the separate ANOVAs for these two intervals did not show a statistically significant difference between the light treatments, the consistent tendency supports a higher g_s in HL for the cultivars. No significant effect of light treatment on mean g_s during the day, or any other analyzed response variable, was found for the diurnal measurements conducted in Experiment 2 (Table 5). Mean g_s was consistently higher in HL for the measured Litago genotypes, however this could also be an effect of the higher light intensity during the day in HL or just a coincidence due to few replicates (as discussed above).

Interestingly, the effect of light treatment on stomatal conductance is here evident during the day, and not at night or during the simulated dawn, when the weak blue light is actually present (Fig. 12 and 16). This suggests that the increased stomatal conductance is not caused by a direct physiological response to the weak blue light. Rather, the high latitude light treatment seems to have induced persistent changes in the leaves resulting in higher g_s during the day when the light conditions in the two treatments were the same (during Experiment 1). A possible explanation is that the additional blue light might have induced developmental changes in the leaf resulting in

higher stomatal density and/or size, and thereby higher stomatal conductance. Changes in stomatal density affect conductance more than altered stomatal length (Lawson & Morison, 2004). Previous experiments with varying proportions of blue in growing light have found increased g_s linked to higher stomatal density and index (number of stomata expressed as per cent of epidermal cells) induced by blue light in several species (Hogewoning et al., 2010; Savvides et al, 2012; Wang et al., 2016; Zheng & Van Labeke, 2017). Also, increased stomatal size in response to monochromatic blue light has been reported in *Solanum lycopersicum* (O'Carrigan et al., 2014). Blue light is known to be involved in light-induced stomatal development, through cryptochrome-mediated signalling in *Arabidopsis* (Kang et al., 2009). No significant effect of light treatment was found on neither density nor lengths of stomata in my results (Table 8 and A.8). However, there is a tendency for higher stomatal density in HL for Milkanova (Fig. 22), which also had the most pronounced difference in g_s found in the point measurements (Fig. 12). While the opposite tendency in stomatal density is found for Finnmark (Fig. 22), which did not seem to have higher stomatal conductance in HL. The known association between blue light and stomatal density makes this a plausible explanation for the observed effect on g_s in this work, although it could not be confirmed by these results.

As described in the introduction, there is considerable interspecific variation in the direct stomatal response to blue light and whether it depends on a background of red light (Matthews et al., 2020). The lack of response to blue light alone has been described in several species (Matthews et al., 2020; Shimazaki et al., 2007). This also seems to be the case for *T. repens* in this work, as no response in g_s is observed when the weak blue light is turned on in LL (Fig. 16). The lack of response is also supported by the low g_s values in the twilight interval (08:30 – 09:30, Fig. 12) and the similar levels of night g_s in the two treatments (the overall mean is even slightly lower in HL, where the blue light is on (Table 5), however the data here is sparse). In contrast, there is a strong response in g_s when the white light is turned on, resulting in a peak before settling at a day-level (Fig. 16).

For all examined plants in both treatments, the g_s peak occurs after the maximum A_n level is reached (Fig. 16 and 17). The A_n level is generally stable from when the plateau is reached in the morning and is not notably affected by the g_s peak, suggesting that A_n

is not limited by g_s when both are at their relatively stable day-level. This indicates that the peak causes unnecessary water-loss (WUE is reduced) in the period from when day-level A_n is reached until g_s has stabilized after the peak. The peaking of g_s can be characterized as stomatal "overshoot", which is a known feature of stomatal opening responses that reduces WUE (McAusland et al., 2016). Stomatal overshoot can result from slow stomatal responses causing continued increase in opening even after the initial signal is removed (Tinoco-Ojanguren & Pearcy, 1993). As there was a brief overlap between the weak blue light and the white growing light in this experiment, these morning overshoots might have been enhanced by the additional blue light in the morning, in both treatments. The results did not show any difference in neither the height of the peak nor the time required to reach it between the light treatments. Whether the pronounced stomatal overshoot observed here is relevant in nature is questionable, as light increases gradually in the morning and is not abruptly switched on as in this experiment. Nonetheless, stomatal overshooting can impact WUE in dynamic light conditions, such as during sun/shade flecks caused by shading leaves or passing clouds (Lawson & Vialet-Chabrand, 2019).

Photosynthetic capacity showed no signs of following the increase in g_s in the high latitude light treatment. Increasing proportions of blue in growing light have been linked to increased photosynthetic capacity associated with higher chlorophyll and N content, as well as lower SLA in other species (Hogewoning et al., 2016; Zheng & Van Labeke, 2017). However, weak blue light at night does not seem to induce these responses in *T. repens*. As explained in Section 2.6.1, the measured photosynthetic assimilation rates cannot be directly compared due to the unfortunate difference in light intensity during the day in Experiment 2. Photosynthetic capacity was not estimated directly but should be associated with the adjusted A_n (A_n/PARi) that was compared here. When A_n was adjusted for light intensity, no difference was found between the treatments (Fig. 18). However, no firm conclusions can be drawn from this due to the small number of replicates. The results from Experiment 1 are more reliable, as the light conditions were then as intended. Chlorophyll content is closely related to, and therefore often used as a proxy for, photosynthetic capacity (Croft et al., 2016). Chlorophyll content was not found to differ between the light treatments (here 27 clones were included per type in each treatment), and this accordingly indicates that photosynthetic capacity was not

substantially affected. Moreover, photosynthetic capacity (per leaf mass), leaf nitrogen concentration and SLA (leaf area/mass) are generally correlated within and between species (Evans, 1989; Reich et al., 1997; Reich et al., 1998; Wright et al., 2004). The close connection between photosynthetic capacity and leaf N is thought to result from the large proportion of N in leaves found in proteins involved in photosynthesis, particularly RuBisCO (ribulose 1-5-bisphosphate oxygenase/carboxylase) (Evans, 1989). The association between photosynthesis and SLA can be explained by diffusional limitation and within-leaf shading in leaves with low SLA (Wright et al., 2004). The leaf N/C ratio tended to be lower in HL, while the tendency was less clear for SLA. No significant effect of light treatment was found for neither, but as only three replicates were included, no firm conclusions can be drawn. Still, taken together there are no signs of increasing photosynthetic activity in HL, and as there is a higher stomatal conductance in HL this suggests a reduced WUE. Ideally, photosynthetic rate and capacity should have been assessed directly in order to establish this.

4.2 Do High Latitude Light Conditions Induce Morphological Effects in *T. repens*?

Significant effects of light treatment were found on all plant growth and architecture variables measured in this study (Table 7; Fig. 21). The pronounced morphological effects of the high latitude light treatment resemble the combination of traits known as shade avoidance syndrome (Smith & Whitelam, 1997). The shade avoidance syndrome is generally characterized by resource allocation to shoot elongation, including extension of internodes and petioles, reduced branching (increased apical dominance), and often retarded leaf development manifested as reduced total leaf area, thinner leaves, and reduced chlorophyll production (Smith & Whitelam, 1997). The response is specific to the shade produced by vegetation, which has a lowered ratio of red to far-red wavelengths (R:FR) and a reduced proportion of blue light, due to the selective absorption of leaf pigments (Franklin, 2008). Shade avoidance is a mechanism by which plants can sense and escape shade from their neighbors, and is considered an important competitive plant strategy (Grime, 1981). There is considerable inter- and intraspecific variation in the response, and it is most pronounced in light demanding plants, so-called shade-avoiders, which *T. repens* is an example of (Christophe et al., 2006).

The role of reduced R:FR in shade-avoidance, through phytochrome signaling, has been well established since the 1970s (Smith & Whitelam, 1997). More recently, low proportions of blue light have been found to induce similar responses as a low R:FR in several species, including *T. repens* (Ballaré & Pierik, 2017; Christophe et al., 2006; Gautier et al., 2001). It seems that the addition of weak blue light at night in this experiment induces similar morphological responses as reduced proportions of blue in growing light in previous studies. In contrast, the observed increase in stomatal conductance (possibly through increased stomatal density) aligns with responses to increasing blue light levels in other studies, as discussed above. However, in this work a weak blue light at night was combined with white growing light during the day, while the mentioned previous studies have tested the effect of a specific light treatment (and mostly higher intensities) during the day (Hogewoning et al., 2010; Savvides et al, 2012; Wang et al., 2016; Zheng & Van Labeke, 2017). Plant responses to light are sensitive to light quality and intensity but can also depend on at what point in the circadian rhythm it is received (Hotta et al., 2017). The light treatment used here is therefore not directly comparable to those of other studies. Nevertheless, the known relationship with blue light is a possible explanation for the responses observed in this work. There was also a small peak in FR wavelengths emitted from the blue light source used (Fig. 4), which may have contributed to the response. However, the R:FR ratio is lower at twilight (Smith & Morgan, 1981), so this should increase the realism of the experiment.

The reduced branching and increased length of stolons, internodes, and petioles found here are consistent with the shade-avoidance syndrome. In contrast, it is less clear whether the observed increase in leaflet size can be attributed to a shade-avoidance response. The effect of shade avoidance on individual leaf area varies between species (Smith & Whitelam, 1997), and Héraut-Bron et al. (2001) found no significant effect of R:FR ratio on individual leaf area in *T. repens*. However, increased area of individual leaves is induced by blue light reduction in several species, and this has also been observed in *T. repens* (Gautier et al., 1997; Varlet-Grancher & Gautier, 1995, as cited in Gautier, 2001). As mentioned, reduced chlorophyll content and thinner leaves (increased SLA) are also characteristic of shade-avoidance responses (Smith & Whitelam, 1997). Neither was found to differ between treatments in this experiment. However, only three replicates per type were included for SLA, so an effect cannot be ruled out. The

underlying mechanisms of the observed morphological effects cannot be inferred from the results of this experiment. Nevertheless, the results show that an extended twilight period can induce a "pseudo-shade-avoidance" in *T. repens*, even with standard growing light during the day.

The observed morphological effects cannot necessarily be extrapolated to field conditions. Latitude is a complex environmental gradient, and many other interacting factors can affect how the responses to light quality may be manifested. For instance, temperature and photoperiod have been shown to affect petiole, internode, and stolon elongation, as well as leaf lamina size in *T. repens* (Junttila et al., 1990). Moreover, light intensity outdoors during the day is several times that of the growing light used in this experiment (Smith & Morgan, 1981). Neither is the light quality or variation in light during the day completely replicated in the laboratory. In an experiment with field plots of *T. repens*, comparing locations in southern and Northern Norway, Aasmo Finne et al. (2000) found significantly lower "foliage height" at the northern location. Due to the prostrate growth habit of *T. repens*, foliage height is likely to be associated with petiole length. Comparing with the results by Aasmo Finne et al. (2000), the increased petiole length observed in this work may thus not be representative to field conditions. However, Aasmo Finne et al. (2000) found better survival of small-leaved and more prostate genotypes at their high-latitude location after a harsh winter in the second year of the experiment, which may partly explain the lower mean foliage height at this location. On the other hand, the main effect of location on leaflet length and internode length was not found to be significant. In line with the difference in winter survival found by Aasmo Finne et al. (2000), wild cold-tolerant *T. repens* populations have been found to have smaller leaves, more numerous plant parts, and being more prostrate than populations from southern Europe (Davies & Young, 1967, as cited in Frame & Newbould, 1986). This could suggest that, if present under field conditions, the morphological responses to extended twilight observed in this thesis (larger leaflets and reduced branching) may contribute to reduced winter hardiness. Higher-yielding, large-leaved and less prostrate southern cultivars of *T. repens*, such as Milkanova, are generally less winter hardy (Helgadóttir et al., 2008). However, the correlation between these traits and winter hardiness might be caused by confounding factors (Helgadóttir et al., 2008). It is thus unclear whether a pseudo-shade-avoidance response to high latitude

light conditions would affect winter survival. Yet, potential effects on the size of leaves and petioles are of particular interest, as this is closely associated with yield in clover (Caradus et al., 1991 as cited in Helgadóttir et al., 2008). Whether the morphological effects observed here could increase yield, through larger leaves and longer petioles, would depend on whether total leaf area or number of leaves are affected. This was not measured, however reduced total leaf area is associated with shade-avoidance in *T. repens* (Christophe et al., 2006). Although there is reason to doubt the pseudo-shade-avoidance response observed in this work would be as evident in field conditions, the results show a response to an aspect of high latitude light conditions that might be relevant for crop development. Therefore, when developing cultivars for high latitudes, field trials could benefit from being carried out at the relevant latitude – and not just at high altitudes further south.

4.3 Do the Selected *T. repens* Types Differ in Their Responses to High Latitude Light Conditions?

The effect of light treatment on g_s level was not shown to differ between the *T. repens* types (Table 4 and 5). However, the Finnmark plants seem to be less affected by the extended twilight. This was most pronounced for the point measurements (Fig. 12 and 13). When it comes to the diurnal measurements, the difference (HL-LL) in mean g_s during the day and night, as well as maximum g_s at the morning peaks, were consistently lower for Finnmark than for the two cultivars (Table 5). As mentioned, this pattern also seems to be reflected in stomatal density (Fig. 22). Moreover, the stomatal responses to changes in light intensity (the time required for stomatal opening and closure) are on average delayed for Finnmark in HL, while they are quicker for the cultivars. These differences between types were not statistically significant, but taken together they indicate that the increased g_s in HL might not apply for Finnmark.

The cultivars seem to have a larger potential for being affected by extended twilight regarding g_s responses. Finnmark differed significantly from Litago, and tended to differ from Milkanova ($p = 0.056$), in the difference in the ratio between mean day g_s to maximum g_s (Table 5). In other words: in HL, the overshoots are increased compared to the day-level g_s for the cultivars, while it is decreased for Finnmark. One possible

interpretation of this is that during the day, the Finnmark plants exploit a relatively higher proportion of their g_s potential (maximum value) in HL. On the other hand, this might as well be a consequence of a higher stomatal overshoot in the morning (and thus higher maximum g_s) in HL for the cultivars, that is not present in Finnmark. The abrupt change in light intensity in this experiment does not represent natural growth conditions. However, McAusland et al. (2016) showed that overshooting stomatal responses can reduce WUE in dynamic light environments. They even suggested rapidity in stomatal responses as a target for improving water use. The results found here could indicate that the cultivars experience more unnecessary water-loss during changes in light intensity when exposed to weak blue light at night, while this is avoided in the Finnmark plants. However, this would need further investigation in order to conclude.

As discussed in the previous section, all three types show a pseudo-shade-avoidance response in the high latitude light treatment. The interaction term Light treatment x Type had no significant effect on size/length of leaflets, petioles, stolons, or internodes (Table 7). This indicates that the types did not differ in their responses for these variables. The response was thus also found in Finnmark, suggesting that the response per se does not hinder survival at high latitudes. However, the types (regardless of treatment) clearly differed in leaflet size and petiole length, with smaller leaves and petioles for Finnmark. The Finnmark plants also had a higher degree of branching, and were thereby typical for high-latitude populations of *T. repens* (Davies & Young, 1967, as cited in Frame & Newbould, 1986). Litago and Milkanova are cultivars that have been artificially selected for higher yield, probably inflating the difference between them and Finnmark. Although all types showed clear morphological responses to the light treatment, the result was more extreme for the cultivars, as they had larger leaves and longer petioles to begin with. On the other hand, Finnmark had the largest response in branching, and all three types differed significantly in this response (significantly different interaction terms, 3.3.1). This is likely, at least partly, a consequence of the difference in architecture between the types: The Finnmark plants are highly branched in general, and they thus have a larger potential for a response in number of branches, while the cultivars have few stolons per plant, also in LL (particularly Litago). In contrast to Milkanova, Litago preforms well in Northern Norway (Graminor, n.d.). However, the high latitude light treatment tested in this work generally produced

similar responses in the two cultivars. The main difference seems to be between these and wild plants originating from a high latitude.

4.4 Do High Latitude Light Conditions Affect Traits Relevant to Earth System Modelling?

Models of stomatal conductance used in the Norwegian Earth System Model (NorESM2) are based on WUE-optimization theory, and stomatal responses to light are modelled as a function of photosynthesis (Section 1.4). The results of this thesis suggest that an extended twilight period may result in sub-optimal WUE, at least for the cultivars. No significant effect of light treatment was found on mean day-time WUE (adjusted for light intensity) based on the diurnal gas exchange measurements (Table 5). However, as discussed in Section 4.1, a significant effect of light treatment was found for midday g_s in the point measurements, where a higher number of replicates were included. The higher g_s found in HL, combined with the lack of any sings of increased photosynthetic rate or capacity (Section 4.1), suggests lower WUE in HL. Additionally, higher stomatal overshoots compared to the day-level g_s may have reduced WUE in the cultivars (Section 4.3). In the Medlyn and Ball-Berry g_s models, light is only included indirectly in terms of the energy in PAR available for photosynthesis (Model details in Appendix A.1). The results of Experiment 1 (Fig. 12) show that low-intensity blue light at night, too low to drive photosynthesis (Fig. 17), has the potential to increase g_s during the day – even though the PAR available for photosynthesis is the same. Accordingly, extended twilight can increase g_s although this cannot be predicted from A_n and PAR.

As discussed in Section 4.3, the increase in g_s is less evident for the Finnmark plants (Fig. 12). This could indicate that a potential sub-optimal WUE caused by extended twilight, is not evident in vegetation native to high latitudes. One could imagine that a sub-optimal WUE in response to the light quality at high latitudes would have been selected against in the native vegetation (at least in environments exposed to drought). However, it has been questioned whether WUE-optimization in it self can constitute an evolutionary advantage (Brodribb et al., 2020). The difference in response between Finnmark and the cultivars regarding WUE may also be an attribute of artificial selection for higher yield in the cultivars, as this is often associated with higher g_s and

reduced WUE (McAusland et al., 2016; Roche, 2015). Although this does not necessarily explain the difference in response to the light treatment. Nevertheless, the results of this work suggest g_s models based on WUE optimization might be less representative at high latitudes, at least in agricultural landscapes – which have the potential to cover larger areas in the future due to climate change (Olesen & Bindi, 2002). Crop-modules may therefore benefit from considering the effects of light conditions at high latitudes. For further investigation, it would be interesting to compare wild plants from different latitudes. If the results are also valid for wild plants originating from lower latitudes, this may also be of increasing relevance due to northward expansion of species ranges in a warmer climate (Parmesan & Yohe, 2003).

Leaf area index (LAI, leaf area per ground area) is also a key parameter in land surface models (Lawrence et al., 2018), and whether it can be affected by high latitude light conditions is therefore interesting in this context. LAI was not measured directly, however it is likely affected considering the observed effects on leaflet area (larger leaves) and internode length (increased distance between leaves) (Fig. 21), although these effects may to some extent cancel each other out. Moreover, reduced total leaf area is often associated with shade-avoidance responses (Smith & Whitelam, 1997), of which all plants in this study showed signs of in HL (Section 4.2). However, in cases when LAI is prescribed based on satellite remote sensing in ESMs, these morphological responses of individual plants are not considered, and would thus not affect the representation of high-latitude vegetation.

The extended twilight period is only one aspect of the light conditions at high latitudes. The light quality during the day is also altered (Bonan, 2016, p. 68), with higher proportions of blue light, in addition to the more extreme seasonal variation in photoperiod. This thesis aimed to study the isolated effect of extended twilight. However, the other unique aspects of high latitude light conditions may also affect gas exchange and morphological responses in plants relevant to ESMs. For further investigation, it would be interesting to also consider the higher proportion of blue light during the day. Previous studies of increased proportions of blue light in growing light has found increased g_s, without a corresponding response in A_n, resulting in lower WUE (Clavijo-Herrera et al.; 2018 Matthews et al., 2020; Shimazaki et al., 2007). In this study, the weak blue light at night did not induce a direct g_s response, probably due to

dependency of red/white background light for the stomatal blue light response (Shimazaki et al., 2007). However, if a higher proportion of blue light was included in growing light during the day, there might be a potential for increased g_s caused by the direct physiological response of stomata. Further investigation in different plant functional types would be needed to evaluate whether these effects are of a relevant magnitude on larger geographical scales, and whether considering these effects of light quality could improve model performance. Nevertheless, this study suggests that the extended twilight at high latitudes has the potential to affect traits of relevance for modelling of vegetation processes.

5 Conclusion

The aim of this thesis was to investigate the effects of the extended twilight period found at high latitudes on gas exchange and morphology in *Trifolium repens*. The responses in controlled growth conditions were compared for three *T. repens* "types": Two cultivars (Milkanova and Litago), and field-collected individuals from Finnmark (collected at $\sim$ 69–70°N).

The artificial extended twilight induced a morphological response resembling shade-avoidance in all three types. This included increased elongation of petioles, internodes and stolons, larger leaflet areas, and reduced branching. For further studies it could be relevant to investigate whether these effects affect yield and winter-hardiness. The results of this work show that an extended twilight period has the potential to affect agriculturally relevant traits. Therefore, when developing cultivars for high latitudes, it may be beneficial to do field trials at the relevant latitude.

Higher stomatal conductance (g_s) was found during the day in the high latitude light treatment (HL, low-intensity blue light at night). However, the weak blue light did not increase stomatal conductance when it was turned on (observed at "dawn" in the low latitude treatment). This suggests that the increased midday g_s in HL was caused by a persistent change in the leaf, possibly increased stomatal density (although this could not be shown here). No effect of light treatment was observed in proxies for photosynthetic capacity. Combined with the increase in g_s, this indicates a reduced water use efficiency (WUE), and an effect on g_s that cannot be predicted from photosynthetic responses to light. This is relevant in the context of Earth System Modelling, as widely used g_s models assume optimal WUE. If the responses observed in this study are also manifested in field conditions, the assumption of optimal WUE might be less representative of high latitude vegetation. However, the increase in g_s was more pronounced in the cultivars and less so in the *T. repens* originating from Finnmark. Thus, this may mainly be relevant for modelling agricultural landscapes at high latitudes, which may cover larger areas in the future due to climate change.

References

Aasmo Finne, M., Rognli, O., & Schjelderup, I. (2000). Genetic variation in a Norwegian germplasm collection of white clover (*Trifolium repens* L.) 1. Population differences in agronomic characteristics. *Euphytica*, *112*(1), 33–44. https://doi.org/10.1023/a:1003818727631

Assmann, S. M., Simoncini, L., & Schroeder, J. I. (1985). Blue light activates electrogenic ion pumping in guard cell protoplasts of *Vicia faba*. *Nature*, *318*(6043), 285–287. https://doi.org/10.1038/318285a0

Assmann, S. M. (1993). Signal transduction in guard cells. *Annual Review of Cell Biology*, *9*(1), 345–375. https://doi.org/10.1146/annurev.cb.09.110193.002021

Ball, J., Woodrow, I., & Berry, J. (1987). A model predicting stomatal conductance and its contribution to the control of photosynthesis under different environmental conditions. In Biggins, J. (Ed.), *Progress in photosynthesis research* (pp. 221–224). Springer. https://doi.org/10.1007/978-94-017-0519-6_48

Ballaré, C. L., & Pierik, R. (2017). The shade-avoidance syndrome: Multiple signals and ecological consequences. *Plant, Cell and Environment*, *40*(11), 2530–2543. https://doi.org/10.1111/pce.12914

Beer, C., Reichstein, M., Tomelleri, E., Ciais, P., Jung, M., Carvalhais, N., Rodenbeck, C., Arain, M. A., Baldocchi, D., Bonan, G. B., Bondeau, A., Cescatti, A., Lasslop, G., Lindroth, A., Lomas, M., Luyssaert, S., Margolis, H., Oleson, K. W., Roupsard, O., ... Papale, D. (2010). Terrestrial gross carbon dioxide uptake: Global distribution and covariation with climate. *Science*, *329*(5993), 834–838. https://doi.org/10.1126/science.1184984

Boggs, S. W. (1931). Seasonal variations in daylight, twilight, and darkness. *Geographical Review*, *21*(4), 656. https://doi.org/10.2307/209373

Bonan, G. (2016). *Ecological Climatology: Concepts and Applications* (3rd ed.). Cambridge University Press.

Brodribb, T. J., Sussmilch, F., & McAdam, S. A. M. (2020). From reproduction to production, stomata are the master regulators. *The Plant Journal*, *101*(4), 756–767. https://doi.org/10.1111/tpj.14561

Buckley, T. N. (2017). Modeling stomatal conductance. *Plant Physiology*, *174*(2), 572–582. https://doi.org/10.1104/pp.16.01772

Christie, J. M. (2007). Phototropin blue-light receptors. *Annual Review of Plant Biology*, *58*(1), 21–45. https://doi.org/10.1146/annurev.arplant.58.032806.103951

Christophe, A., Moulia, B., & Varlet-Grancher, C. (2006). Quantitative contributions of blue light and par to the photocontrol of plant morphogenesis in *Trifolium repens* (l.) *Journal of Experimental Botany*, *57*(10), 2379–2390. https://doi.org/10.1093/jxb/erj210

Clavijo-Herrera, J., Van Santen, E., & Gómez, C. (2018). Growth, water-use efficiency, stomatal conductance, and nitrogen uptake of two lettuce cultivars grown under different percentages of blue and red light. *Horticulturae*, *4*(3). https://doi.org/10.3390/horticulturae4030016

Cowan, I. R., & Farquhar, G. D. (1977). Stomatal function in relation to leaf metabolism and environment. *Symposia of the Society for Experimental Biology*, *31*, 471–505.

Croft, H., Chen, J. M., Luo, X., Bartlett, P., Chen, B., & Staebler, R. M. (2017). Leaf chlorophyll content as a proxy for leaf photosynthetic capacity. *Global Change Biology*, *23*(9), 3513–3524. https://doi.org/10.1111/gcb.13599

Department of Geosciences, University of Oslo. (2019). *EMERALD – Terrestrial ecosystem–climate interactions of our EMERALD planet* [Accessed: 2022-04-12]. https://www.mn.uio.no/geo/english/research/projects/emerald/

Ehleringer, J., & Sandquist, D. R. (2018). Photosynthesis: Physiological and ecological considerations. In L. Taiz, E. Zeiger, I. M. Møller, & A. Murphy (Eds.), *Plant physiology and development* (International Sixth, pp. 245–267). Oxford University Press.

Evans, J. R. (1989). Photosynthesis and nitrogen relationships in leaves of C_3 plants. *Oecologia*, *78*(1), 9–19. https://doi.org/10.1007/bf00377192

Farquhar, G., von Caemmerer, S., & Berry, J. (1980). A biochemical model of photosynthetic CO_2 assimilation in leaves of C_3 species. *Planta*, *149*, 78–90. https://doi.org/10.1007/BF00386231

Frame, J., & Newbould, P. (1986). Agronomy of white clover. In Brady, N.C. (Ed.), *Advances in Agronomy* (pp. 1–88). Academic Press. https://doi.org/10.1016/S0065-2113(08)60280-1

Franks, P. J., Berry, J. A., Lombardozzi, D. L., & Bonan, G. B. (2017). Stomatal function across temporal and spatial scales: Deep-time trends, land-atmosphere coupling

and global models. *Plant Physiology*, *174*(2), 583–602. https://doi.org/10.1104/pp.17.00287

Franks, P. J., Bonan, G. B., Berry, J. A., Lombardozzi, D. L., Holbrook, N. M., Herold, N., & Oleson, K. W. (2018). Comparing optimal and empirical stomatal conductance models for application in earth system models. *Global Change Biology*, *24*(12), 5708–5723. https://doi.org/10.1111/gcb.14445

Gago, J., Daloso, D. D. M., Figueroa, C. M., Flexas, J., Fernie, A. R., & Nikoloski, Z. (2016). Relationships of leaf net photosynthesis, stomatal conductance, and mesophyll conductance to primary metabolism: A multispecies meta-analysis approach. *Plant Physiology*, *171*(1), 265–279. https://doi.org/10.1104/pp.15.01660

Gautier, H., Varlet-Grancher, C., & Membré, J. M. (2001). Plasticity of petioles of white clover (*Trifolium repens*) to blue light. *Physiologia Plantarum*, *112*(2), 293–300. https://doi.org/10.1034/j.1399-3054.2001.1120219.x

Gitelson, A. A., Buschmann, C., & Lichtenthaler, H. K. (1999). The chlorophyll fluorescence ratio f735/f700 as an accurate measure of the chlorophyll content in plants. *Remote Sensing of Environment*, *69*(3), 296–302. https://doi.org/10.1016/s0034-4257(99)00023-1

Global Invasive Species Database (GISD). (2010). Species profile: *Trifolium repens* [Accessed: 2022-04-10]. http://www.iucngisd.org/gisd/species.php?sc=1608

Graminor. (n.d.). *Litago* [Accessed: 2022-03-25]. https://graminor.no/sort/litago/

Grime, J. P. (1981). Plant strategies in shade. In H. Smith (Ed.), *Plants and the daylight spectrum* (pp. 159–186). Academic Press.

Helgadóttir, Á., Marum, P., Dalmannsdóttir, S., Daugstad, K., Kristjánsdóttir, T. A., & Lunnan, T. (2008). Combining winter hardiness and forage yield in white clover (*Trifolium repens*) cultivated in northern environments. *Annals of Botany*, *102*, 25–834, 2. https://doi.org/10.1093/aob/mcn159

Héraut-Bron, V., Robin, C., Varlet-Grancher, C., & Guckert, A. (2001). Phytochrome mediated effects on leaves of white clover: Consequences for light interception by the plant under competition for light. *Annals of Botany*, *88*(4), 737–743. https://doi.org/10.1006/anbo.2001.1510

Hogewoning, S. W., Trouwborst, G., Maljaars, H., Poorter, H., van Ieperen, W., & Harbinson, J. (2010). Blue light dose–responses of leaf photosynthesis, morphology, and

chemical composition of *Cucumis sativus* grown under different combinations of red and blue light. *Journal of Experimental Botany*, *61*(11), 3107–3117. https://doi.org/10.1093/jxb/erq132

Hotta, C. T., Gardner, M. J., Hubbard, K. E., Baek, S. J., Dalchau, N., Suhita, D., Dodd, A. N., & Webb, A. A. R. (2007). Modulation of environmental responses of plants by circadian clocks. *Plant, Cell and Environment*, *30*(3), 333–349. https://doi.org/10.1111/j.1365-3040.2006.01627.x

Huché-Thélier, L., Crespel, L., Gourrierec, J. L., Morel, P., Sakr, S., & Leduc, N. (2016). Light signaling and plant responses to blue and uv radiations—perspectives for applications in horticulture. *Environmental and Experimental Botany*, *121*, 22–38. https://doi.org/10.1016/j.envexpbot.2015.06.009

Inoue, S.-i., Takemiya, A., & Shimazaki, K.-i. (2010). Phototropin signaling and stomatal opening as a model case. *Current Opinion in Plant Biology*, *13*(5), 587–593. https://doi.org/10.1016/j.pbi.2010.09.002

Junttila, O., Svenning, M. M., & Solheim, B. (1990). Effects of temperature and photoperiod on vegetative growth of white clover (*Trifolium repens*) ecotypes. *Physiologia Plantarum*, *79*(3), 427–434. https://doi.org/10.1111/j.1399-3054.1990.tb02098.x

Kang, C.-Y., Lian, H.-L., Wang, F.-F., Huang, J.-R., & Yang, H.-Q. (2009). Cryptochromes, phytochromes, and COP1 regulate light-controlled stomatal development in *Arabidopsis*. *The Plant Cell*, *21*(9), 2624–2641. https://doi.org/10.1105/tpc.109.069765

Karlsson, P. E. (1986). Blue light regulation of stomata in wheat seedlings. I. Influence of red background illumination and initial conductance level. *Physiologia Plantarum*, *66*, 202–206. https://doi.org/10.1111/j.1399-3054.1986.tb02409.x

Kinoshita, T. (1999). Blue light activates the plasma membrane H^+-ATPase by phosphorylation of the C-terminus in stomatal guard cells. *The EMBO Journal*, *18*(20), 5548–5558. https://doi.org/10.1093/emboj/18.20.5548

Kinoshita, T., Doi, M., Suetsugu, N., Kagawa, T., Wada, M., & Shimazaki, K.-i. (2001). Phot1 and phot2 mediate blue light regulation of stomatal opening. *Nature*, *414*(6864), 656–660.

Klüsener, B., Young, J. J., Murata, Y., Allen, G. J., Mori, I. C., Hugouvieux, V., & Schroeder, J. I. (2002). Convergence of calcium signaling pathways of pathogenic

elicitors and abscisic acid in *Arabidopsis* guard cells. *Plant Physiology*, *130*(4), 2152–2163. https://doi.org/10.1104/pp.012187

Lawrence, D., Fisher, R., Koven, C., Oleson, K., Swenson, S., Vertenstein, M., Andre, B., Bonan, G., Ghimire, B., Kampenhout, L., Kennedy, D., Kluzek, E., Knox, R., Lawrence, P., Li, F., Li, H., Lombardozzi, D., Lu, Y., Perket, J., ... Zeng, X. (2018). *Technical description of version 5.0 of the community land model (clm)* [Accessed: 2021-05-24]. https://www.cesm.ucar.edu/models/cesm2/land/CLM50_Tech_Note.pdf

Lawson, T., & Blatt, M. R. (2014). Stomatal size, speed, and responsiveness impact on photosynthesis and water use efficiency. *Plant Physiology*, *164*(4), 1556–1570. https://doi.org/10.1104/pp.114.237107

Lawson, T., & Morison, J. (2004). Stomatal function and physiology. In A. R. Hemsley & I. Poole (Eds.), *The evolution of plant physiology* (pp. 217–242). Academic Press.

Lawson, T., & Vialet-Chabrand, S. (2019). Speedy stomata, photosynthesis and plant water use efficiency. *New Phytologist*, *221*(1), 93–98. https://doi.org/10.1111/nph.15330

Lichtenthaler, H. K. (1987). Chlorophylls and carotenoids: Pigments of photosynthetic biomembranes. Elsevier Science; Technology. https://doi.org/10.1016/0076-6879(87)48036-1

LI-COR Biosciences. (2012). *Using the li-6400/li-6400xt portable photosynthesis system, version 6*. LI-COR Biosciences. Lincoln, Nebraska, U.S.A.

Liland, K. H. (2021). *Mixlm: Mixed model anova and statistics for education* [R package version 1.2.5]. https://CRAN.R-project.org/package=mixlm

Matthews, J. S. A., & Lawson, T. (2019). Climate change and stomatal physiology. *Annual Plant Reviews Online*, 713–752. https://doi.org/10.1002/9781119312994.apr0667

Matthews, J. S. A., Vialet-Chabrand, S., & Lawson, T. (2020). Role of blue and red light in stomatal dynamic behaviour. *Journal of Experimental Botany*, *71*(7), 2253–2269. https://doi.org/10.1093/jxb/erz563

McAusland, L., Vialet-Chabrand, S., Davey, P., Baker, N. R., Brendel, O., & Lawson, T. (2016). Effects of kinetics of light-induced stomatal responses on photosynthesis and water-use efficiency. *New Phytologist*, *211*(4), 1209–1220. https://doi.org/10.1111/nph.14000

Medlyn, B. E., Duursma, R. A., Eamus, D., Ellsworth, D. S., Prentice, I. C., Barton, C. V. M., Crous, K. Y., De Angelis, P., Freeman, M., & Wingate, L. (2011). Reconciling the optimal and empirical approaches to modelling stomatal conductance. *Global Change Biology*, *17(6)*, 2134–2144. https://doi.org/10.1111/j.1365-2486.2010.02375.x

Medlyn, B. E., Duursma, R. A., Eamus, D., Ellsworth, D. S., Prentice, I. C., Barton, C. V. M., Crous, K. Y., De Angelis, P., Freeman, M., & Wingate, L. (2012). Reconciling the optimal and empirical approaches to modelling stomatal conductance. *Global Change Biology*, *18*, 3476–3476. https://doi.org/10.1111/j.1365-2486.2012.02790.x

Meziane, D., & Shipley, B. (2001). Direct and indirect relationships between specific leaf area, leaf nitrogen and leaf gas exchange. Effects of irradiance and nutrient supply. *Annals of Botany*, *88*(5), 915–927. https://doi.org/10.1006/anbo.2001.1536

O'Carrigan, A., Babla, M., Wang, F., Liu, X., Mak, M., Thomas, R., Bellotti, B., & Chen, Z.-H. (2014). Analysis of gas exchange, stomatal behaviour and micronutrients uncovers dynamic response and adaptation of tomato plants to monochromatic light treatments. *Plant Physiology and Biochemistry*, *82*, 105–115. https://doi.org/10.1016/j.plaphy.2014.05.012

Olesen, J. E., & Bindi, M. (2002). Consequences of climate change for European agricultural productivity, land use and policy. *European Journal of Agronomy*, *16*(4), 239–262. https://doi.org/10.1016/s1161-0301(02)00004-7

Parmesan, C., & Yohe, G. (2003). A globally coherent fingerprint of climate change impacts across natural systems. *Nature*, *421*(6918), 37–42. https://doi.org/10.1038/nature01286

R Core Team. (2021). *R: A language and environment for statistical computing*. R Foundation for Statistical Computing. Vienna, Austria. https://www.R-project.org/

Reich, P. B., Ellsworth, D. S., & Walters, M. B. (1998). Leaf structure (specific leaf area) modulates photosynthesis-nitrogen relations: Evidence from within and across species and functional groups. *Functional Ecology*, *12*(6), 948–958. https://doi.org/10.1046/j.1365-2435.1998.00274.x

Reich, P. B., Walters, M. B., & Ellsworth, D. S. (1997). From tropics to tundra: Global convergence in plant functioning. *Proceedings of the National Academy of Sciences*, *94*(25), 13730–13734. https://doi.org/10.1073/pnas.94.25.13730

Roche, D. (2015). Stomatal conductance is essential for higher yield potential of c_3 crops. *Critical Reviews in Plant Sciences*, *34*(4), 429–453. https://doi.org/10.1080/07352689.2015.1023677

Rogers, A., Medlyn, B. E., Dukes, J. S., Bonan, G., Caemmerer, S., Dietze, M. C., Kattge, J., Leakey, A. D. B., Mercado, L. M., Niinemets, Ü., Prentice, I. C., Serbin, S. P., Sitch, S., Way, D. A., & Zaehle, S. (2017). A roadmap for improving the representation of photosynthesis in earth system models. *New Phytologist*, *213*(1), 22–42. https://doi.org/10.1111/nph.14283

Savvides, A., Fanourakis, D., & Van Ieperen, W. (2012). Co-ordination of hydraulic and stomatal conductances across light qualities in cucumber leaves. *Journal of Experimental Botany*, *63*(3), 1135–1143. https://doi.org/10.1093/jxb/err348

Schindelin, J., Arganda-Carreras, I., Frise, E., Kaynig, V., Longair, M., Pietzsch, T., Preibisch, S., Rueden, C., Saalfeld, S., Schmid, B., Tinevez, J.-Y., White, D. J., Hartenstein, V., Eliceiri, K., Tomancak, P., & Cardona, A. (2012). Fiji: An open-source platform for biological-image analysis. *Nature Methods*, *9*(7), 676–682. https://doi.org/10.1038/nmeth.2019

Schlesinger, W. H., & Bernhardt, E. S. (2013). *Biogeochemistry, an analysis of global change* (Third). Academic Press.

Schroeder, J. I., Raschke, K., & Neher, E. (1987). Voltage dependence of K^+ channels in guard-cell protoplasts. *84*(12), 4108–4112. https://doi.org/10.1073/pnas.84.12.4108

Seland, Ø., Bentsen, M., Olivié, D., Toniazzo, T., Gjermundsen, A., Graff, L. S., Debernard, J. B., Gupta, A. K., He, Y.-C., Kirkevåg, A., Schwinger, J., Tjiputra, J., Aas, K. S., Bethke, I., Fan, Y., Griesfeller, J., Grini, A., Guo, C., Ilicak, M., ... Schulz, M. (2020). Overview of the Norwegian Earth System Model (NorESM2) and key climate response of CMIP6 DECK, historical, and scenario simulations. *Geoscientific Model Development*, *13*(12), 6165–6200. https://doi.org/10.5194/gmd-13-6165-2020

Shimazaki, K.-I., Doi, M., Assmann, S. M., & Kinoshita, T. (2007). Light regulation of stomatal movement. *Annual Review of Plant Biology*, *58*(1), 219–247. https://doi.org/10.1146/annurev.arplant.57.032905.105434

Smith, H., & Morgan, D. C. (1981). The spectral characteristics of the visible radiation incident upon the surface of the earth. In H. Smith (Ed.), *Plants and the daylight spectrum* (pp. 5–20). Academic Press.

Smith, H., & Whitelam, G. C. (1997). The shade avoidance syndrome: Multiple responses mediated by multiple phytochromes. *Plant, Cell and Environment*, *20*(6), 840–844. https://doi.org/10.1046/j.1365-3040.1997.d01-104.x

Talbott, L. D., & Zeiger, E. (1996). Central roles for potassium and sucrose in guard-cell osmoregulation. *Plant Physiology*, *111*(4), 1051–1057. https://doi.org/10.1104/pp.111.4.1051

Tinoco-Ojanguren, C., & Pearcy, R. W. (1993). Stomatal dynamics and its importance to carbon gain in two rainforest piper species. I. VPD effects on the transient stomatal response to lightflecks. *Oecologia*, *94*(3), 388–394. http://www.jstor.org/stable/4220366

Walker, A. P., Beckerman, A. P., Gu, L., Kattge, J., Cernusak, L. A., Domingues, T. F., Scales, J. C., Wohlfahrt, G., Wullschleger, S. D., & Woodward, F. I. (2014). The relationship of leaf photosynthetic traits - V_{cmax} and J_{max} - to leaf nitrogen, leaf phosphorus, and specific leaf area: A meta-analysis and modeling study. *Ecology and Evolution*, *4*(16), 3218–3235. https://doi.org/10.1002/ece3.1173

Wang, J., Lu, W., Tong, Y., & Yang, Q. (2016). Leaf morphology, photosynthetic performance, chlorophyll fluorescence, stomatal development of lettuce (*Lactuca sativa* L.) exposed to different ratios of red light to blue light. *Frontiers in Plant Science*, *7*. https://doi.org/10.3389/fpls.2016.00250

Willmer, C. M., & Fricker, M. (1996). *Stomata* (2nd ed.). Chapman; Hall.

Wong, S. C., Cowan, I. R., & Farquhar, G. D. (1979). Stomatal conductance correlates with photosynthetic capacity. *Nature (London)*, *282*(5737), 424–426. https://doi.org/10.1038/282424a0

Wright, I. J., Reich, P. B., Westoby, M., Ackerly, D. D., Baruch, Z., Bongers, F., Cavender-Bares, J., Chapin, T., Cornelissen, J. H. C., Diemer, M., Flexas, J., Garnier, E., Groom, P. K., Gulias, J., Hikosaka, K., Lamont, B. B., Lee, T., Lee, W., Lusk, C.,

... Villar, R. (2004). The worldwide leaf economics spectrum. *Nature*, *428*(6985), 821–827. https://doi.org/10.1038/nature02403

Zeiger, E. (2018). Stomatal biology. In L. Taiz, E. Zeiger, I. M. Møller, & A. Murphy (Eds.), *Plant physiology and development* (International Sixth, pp. 285–316). Oxford University Press.

Zeiger, E., Field, C., & Mooney, H. A. (1981). Stomatal opening at dawn: Possible roles of the blue light response in nature. In H. Smith (Ed.), *Plants and the daylight spectrum* (pp. 391–407). Academic Press.

Zeiger, E., & Hepler, P. K. (1977). Light and stomatal function: Blue light stimulates swelling of guard cell protoplasts. *Science*, *196*(4292), 887–889.

Zeiger, E., & Field, C. (1982). Photocontrol of the functional coupling between photosynthesis and stomatal conductance in the intact leaf. *Plant Physiology*, *70*(2), 370–375. https://doi.org/10.1104/pp.70.2.370

Zheng, L., & Labeke Van, M.-C. (2017). Long-term effects of red- and blue-light emitting diodes on leaf anatomy and photosynthetic efficiency of three ornamental pot plants. *Frontiers in Plant Science*, *8*. https://doi.org/10.3389/fpls.2017.00917

Zoric, L., Merkulov, L., Lukovic, J., Boza, P., & Polic, D. (2009). Leaf epidermal characteristics of *Trifolium* L. species from Serbia and Montenegro. *Flora - Morphology, Distribution, Functional Ecology of Plants*, *204*(3), 198–209. https://doi.org/10.1016/j.flora.2008.02.002

A Appendix

A.1 Models of Stomatal Conductance

The Ball-Berry model represents stomatal conductance to water vapor (g_s) as a function of photosynthetic assimilation rate (A_n) with empirically estimated parameters (Ball et al., 1987; Bonan, 2016):

$$g_s = g_0 + g_1 A_n \frac{h_s}{c_s} ,$$

where g_0 is the minimum conductance, g_1 is an empirically estimated stomatal slope, c_s is CO_2 concentration at the leaf surface, and h_s is the relative humidity at the leaf surface (h_s has in later versions been replaced by functions of vapor pressure deficit).

The Medlyn model (Medlyn et al., 2011; Medlyn et al., 2012) calculates stomatal conductance as:

$$g_s = g_o + 1.6(1 + \frac{g_1}{\sqrt{D}})\frac{A_n}{c_s}$$

where D is vapor pressure deficit at the leaf surface (in kPa when g_1 is in $\text{kPa}^{0.5}$), and 1.6 is a conversion factor adjusting for the higher diffusion rate of H_2O compared to CO_2.

In both the Ball-Berry and the Medlyn Model, A_n is given by the Farquhar-Caemmerer-Berry photosynthesis model (Farquhar et al., 1980), in which A_n is determined by the limiting of two rates: The Rubisco-limited rate, A_c, or the light-limited rate, A_j. A_j is a function of electron transport rate in photosystem II, which varies with absorbed PAR (Lawrence et al., 2018). Later model updates has added a third possibly limiting rate: Triose phosphate utilisation, A_p, the rate at which the primary products of photosynthesis is consumed or converted by the plant (Bonan, 2016). Including all three rates, the photosynthesis model can be expressed as:

$$A_n = min(A_c, A_j, A_p) - R_d$$

Where A_n is the net assimilation rate, and R_d is the respiration rate. Photosynthesis and stomatal conductance can be modelled by solving the corresponding equations iteratively.

A.2 Plant Material

Table A.1: Details for field collection of Finnmark *Trifolium repens*. The plants were collected for a previous project, at four locations in Finnmark (Northern Norway).

Genotype	Location	Coordinates	Date	Collector
ON 1 – 4	Øvre Neiden	69.69823°N, 29.27277°E	24.10.2018	Ane V. Vollsnes
45 – 49	Karasjok	69.46900°N, 25.50787°E	22.08.2017	Aud E. B. Eriksen
18	Svanvik	69.44517°N, 30.05202°E	30.07.2017	Aud E. B. Eriksen
213	Alta	69.95931°N, 23.29695°E	26.09.2017	Roar Haug

A.3 Growth Conditions

Table A.2: Overview of spraying events. Spraying was conducted before Experiment 1 and between Experiment 1 and 2, by Ingrid Johansen and Marit Langrekken.

Date	Insecticide
15.02.2021	Conserve SC, Dow AgroSciences, Zionsville, IN, US
22.02.2021	Decis Options, Bayer AG, Leverkusen, Germany
30.06.2021	Vermitec, Syngenta, Basel, Switzerland
06.07.2021	Vermitec, Syngenta, Basel, Switzerland
13.07.2021	Decis Options, Bayer AG, Leverkusen, Germany

A.4 Chlorophyll a Standard Curve

A.4.1 Calculations: Dilution of Chlorophyll a Standard

The concentrations of chlorophyll a standard in each dilution step was calculated from the relationship,

$$c_a V_a = c_b V_b \tag{3}$$

between a solution before (b) and after (a) dilution, where $c_{a/b}$ and $V_{a/b}$ are the concentration and volume of solution a/b. Starting with 0.1 mg chlorophyll a/mL (Sigma-Aldrich Chlorophyll a analytical standard, article no. 96145), a four-step serial dilution, with 96 % ethanol, was done accordingly:

$$c_1 = \frac{0.10\ {}^{mg}/_{mL} * 0.30\ mL}{3.3\ mL} = 9.09\ {}^{\mu g}/_{mL}$$

$$c_2 = \frac{c_1 * 0.30\ mL}{3.3\ mL} = 0.83\ {}^{\mu g}/_{mL}$$

$$c_3 = \frac{c_2 * 0.30\ mL}{3.3\ mL} = 0.075\ {}^{\mu g}/_{mL}$$

$$c_4 = \frac{c_3 * 0.30\ mL}{3.3\ mL} = 0.0068\ {}^{\mu g}/_{mL}$$

where c_1 – c_4 are the resulting concentrations of the standard solutions. For each step, 0.30 mL of the previous solution in the series was added to 3 mL 96% ethanol. Therefore, $V_b = 0.30\ mL$ and $V_a = 3.3\ mL$ in each step.

A.4.2 Standard Curve and Tables

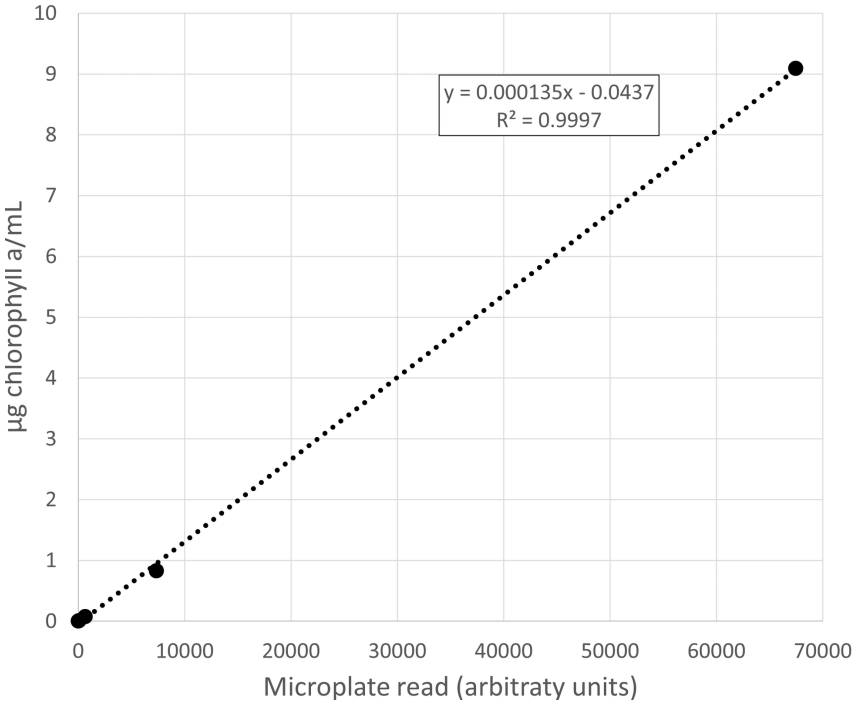

Figure A.1: Standard curve relating microplate reads to chlorophyll a concentration, based on a four-step serial dilution of Sigma-Aldrich Chlorophyll a analytical standard (known concentrations). The points shown are averages of three repeated measurements. This linear model (y = 0.000135x - 0.0437) was used to convert microplate reads to chlorophyll a concentration in the wells with leaf sample extracts.

Table A.3: Results of chemical analysis of chlorophyll content, used to construct the standard curve shown in Figure 8. There are three replicate leaf samples for each genotype included. Genotypes labeled "ON" and "V" are Finnmark, while Milkanova and Litago are abbreviated "M" and "L". Average well reads are averages of three repeated measurements (Table A.4).

Leaf sample	Average well read	Chl. a concentration in well (µg/ml)	Leaf sample area	Chl. a concentration before dilution (µg/ml)	Chl. a per leaf area (µg/cm^2)	CCM-300 read
V47.1	19641.7	2.61	1.48	52.2	49.3	338
V47.2	20066.3	2.67	1.22	53.3	61.3	332
V47.3	9871.7	1.29	0.73	25.8	49.4	357
V45.1	10743.7	1.41	0.64	28.1	62.0	370
V45.2	16423.7	2.17	0.84	43.5	72.4	408
V45.3	7685.3	0.99	0.50	19.9	56.1	344
ON1.1	13820.7	1.82	0.62	36.4	82.2	471
ON1.2	20642.0	2.74	0.95	54.9	81.3	439
ON1.3	14741.3	1.95	0.87	38.9	62.6	401
ON4.1	10603.3	1.39	0.49	27.8	79.5	465
ON4.2	19180.3	2.55	0.80	50.9	88.8	452
ON4.3	9062.3	1.18	0.50	23.6	66.2	401
M4.1	12052.3	1.58	0.93	31.7	47.5	338
M4.2	8254.7	1.07	0.52	21.4	57.2	439
M4.3	9748.0	1.27	0.57	25.4	62.4	408
M5.1	28630.0	3.82	1.89	76.4	56.5	376
M5.2	16956.0	2.25	0.94	44.9	67.0	439
M5.3	12093.0	1.59	1.00	31.8	44.4	351
M9.1	8591.0	1.12	0.68	22.3	45.7	306
M9.2	11278.7	1.48	1.00	29.6	41.5	325
M9.3	13278.3	1.75	0.85	35.0	57.7	363
L29.1	27027.7	3.61	1.43	72.1	70.8	376
L29.2	10502.3	1.37	0.55	27.5	69.7	414
L29.3	15909.0	2.10	1.22	42.1	48.3	300
L30.1	18240.0	2.42	1.08	48.4	62.8	395
L30.2	14455.3	1.91	0.92	38.2	58.0	408
L30.3	13558.7	1.79	0.79	35.7	63.6	433
L33.1	19808.7	2.63	1.12	52.6	65.5	401
L33.2	18710.0	2.48	1.03	49.6	67.3	325
L33.3	29350.3	3.92	1.33	78.4	82.4	370

Table A.4: Microplate reads for chemical analysis of chlorophyll content. There are three replicate leaf samples for each genotype included, and three repeated measurements for each replicate. Genotypes labeled "ON" and "V" are Finnmark, while Milkanova and Litago are abbreviated "M" and "L".

Sample	Well Read
V47.1	19566
V47.1	19655
V47.1	19704
V47.2	19533
V47.2	20185
V47.2	20481
V47.3	9932
V47.3	9767
V47.3	9916
V45.1	10634
V45.1	10757
V45.1	10840
V45.2	16173
V45.2	16525
V45.2	16573
V45.3	7281
V45.3	7810
V45.3	7965
ON1.1	13347
ON1.1	13844
ON1.1	14271
ON1.2	20591
ON1.2	20846
ON1.2	20489
ON1.3	14789
ON1.3	14679
ON1.3	14756
ON4.1	10202
ON4.1	10885
ON4.1	10723

Sample	Well Read
ON4.2	18742
ON4.2	19433
ON4.2	19366
ON4.3	8900
ON4.3	9213
ON4.3	9074
M4.1	11903
M4.1	12288
M4.1	11966
M4.2	7922
M4.2	8377
M4.2	8465
M4.3	9416
M4.3	9703
M4.3	10125
M5.1	27937
M5.1	28842
M5.1	29111
M5.2	16822
M5.2	17047
M5.2	16999
M5.3	11748
M5.3	12174
M5.3	12357
M9.1	8504
M9.1	8635
M9.1	8634
M9.2	11103
M9.2	11381
M9.2	11352

Sample	Well Read
M9.3	12989
M9.3	13500
M9.3	13346
L29.1	26430
L29.1	27686
L29.1	26967
L29.2	10171
L29.2	10581
L29.2	10755
L29.3	15462
L29.3	15990
L29.3	16275
L30.1	18620
L30.1	17855
L30.1	18245
L30.2	14026
L30.2	14615
L30.2	14725
L30.3	13674
L30.3	12945
L30.3	14057
L33.1	19508
L33.1	20280
L33.1	19638
L33.2	18565
L33.2	18707
L33.2	18858
L33.3	29244
L33.3	29475
L33.3	29332

A.5 Morphological Measurements

A.5.1 Leaflet Vein as a Proxy for Leaflet Area

In order to evaluate the use of squared leaflet vein length as a proxy for leaflet area, leaflet area was measured and compared to squared leaflet vein length for 18 leaves. These were leaves from three genotypes of each type, from both light treatments. Each leaf was photographed on red millimeter paper, and area and vein length were determined from the images using Fiji software. As the leaflet shape was similar across the three types, the relationship between squared vein length and area was assumed to be equal. There was a clear positive relationship ($R^2 = 0.854$), justifying the proxy measurement (Fig. A.2).

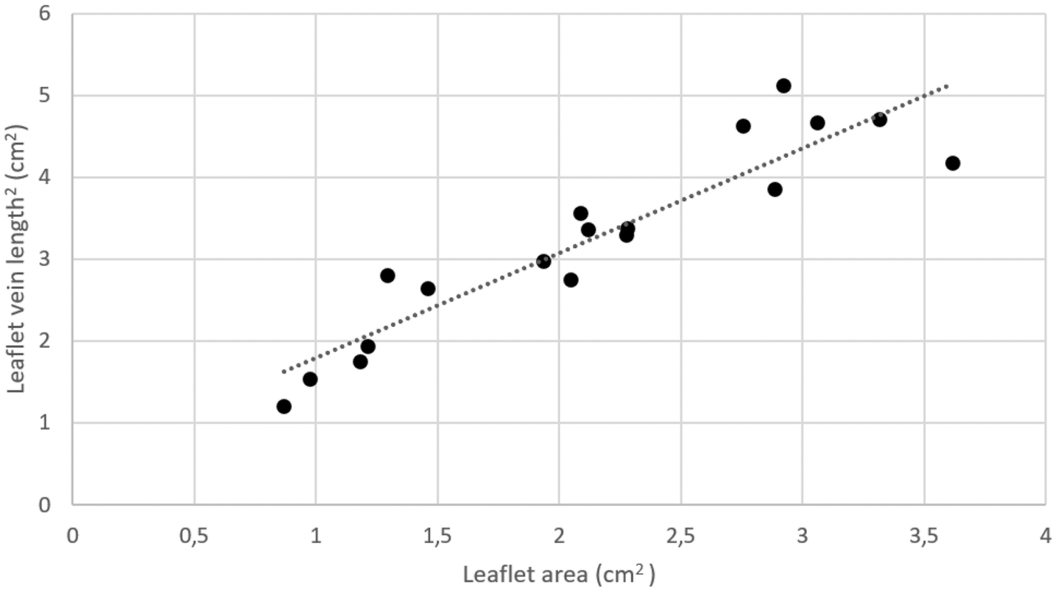

Figure A.2: Squared leaflet vein length as a proxy for leaflet area. Leaflet area was measured and compared to the squared leaflet length on the same leaflets, for a sub-sample of three genotypes of each type, from both light treatments. There was a strong positive correlation ($R^2 = 0.854$), justifying the use of squared leaflet vein length as a proxy for leaflet area.

A.6 Model Adequacy Checking

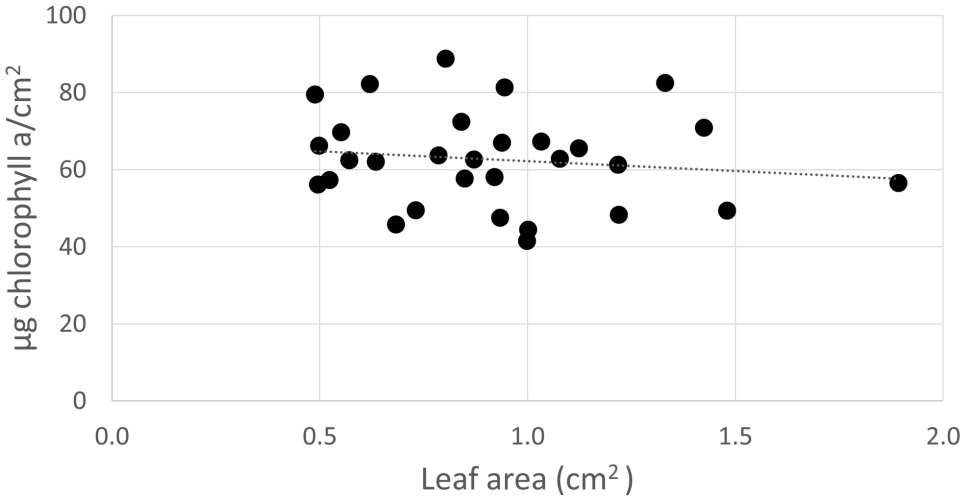

Figure A.3: Chlorophyll content plotted against the area of the leaf sample from which it was extracted, to assess whether sample size affected the extraction. There seems to be no correlation between the two ($R^2 = 0.0196$).

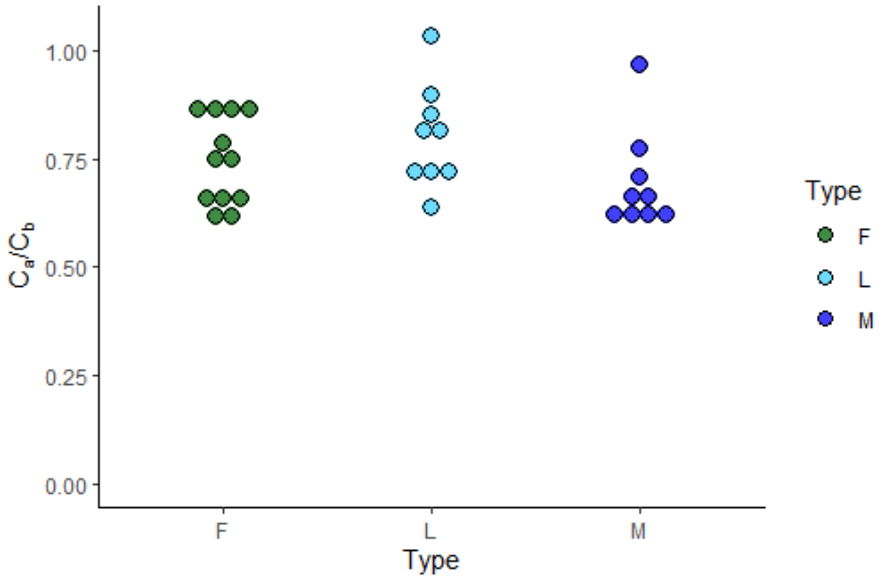

Figure A.4: Ratio of chlorophyll a to chlorophyll b, three leaves were sampled from each of three Litago and Milkanova genotypes, and four Finnmark genotypes. F = Finnmark, M = Milkanova, L = Litago.

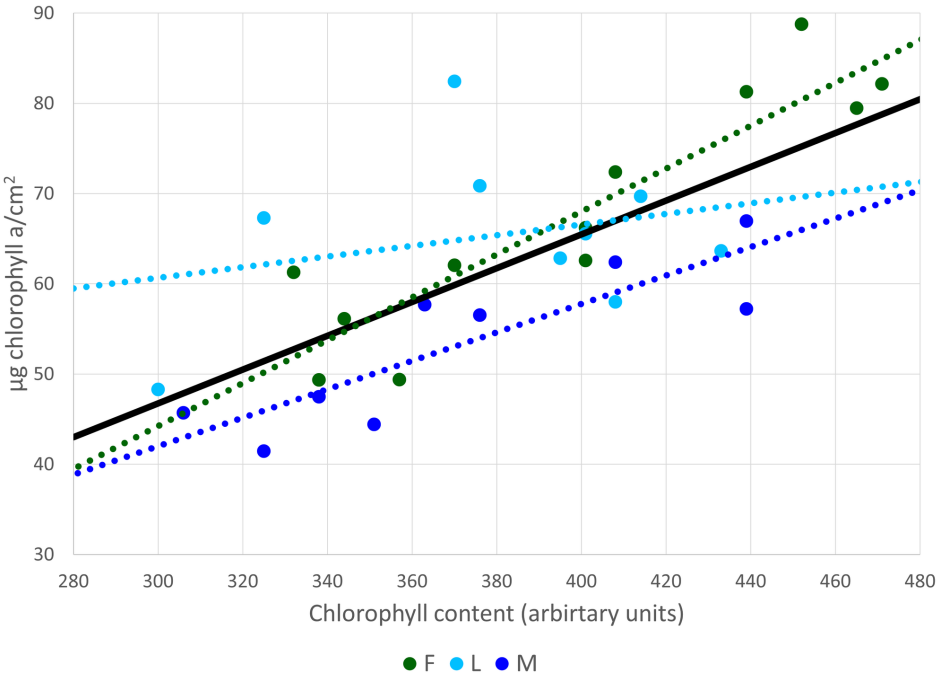

Figure A.5: Standard curves relating absolute chlorophyll content ($\mu g/cm^2$), determined using the microplate reader, and CCM-reads (for the same leaf samples). The common model, shown in black, was used, as separate models for each type did not differ significantly. F = Finnmark, M = Milkanova, L = Litago.

Table A.5: 95% confidence intervals for slope of linear models of the standard curves shown in Figure A.5. As their confidence intervals overlap, a common model ("Total") was used for the three types.

Type	95% C.I. for Regression Coefficient
Finnmark	0.161, 0.315
Litago	-0.127, 0.245
Milkanova	0.0734, 0.242
Total	0.118, 0.256

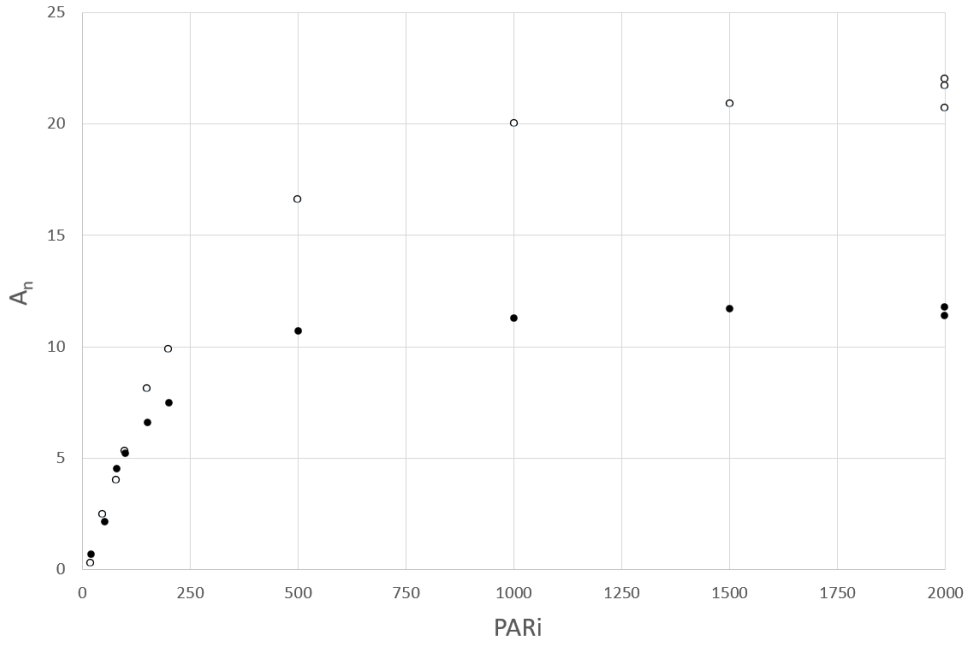

Figure A.6: Light response curves for two genotypes of Finnmark *Trifolium repens*, made by Ane Victoria Vollsnes for a previous project, using the LI6400 portable photosynhtesis system. A_n = net photosynthetic rate (µmol CO_2/m^2s), PARi = photosynthetic photon flux density (µmol photons m^{-2} s^{-1}) in the leaf chamber.

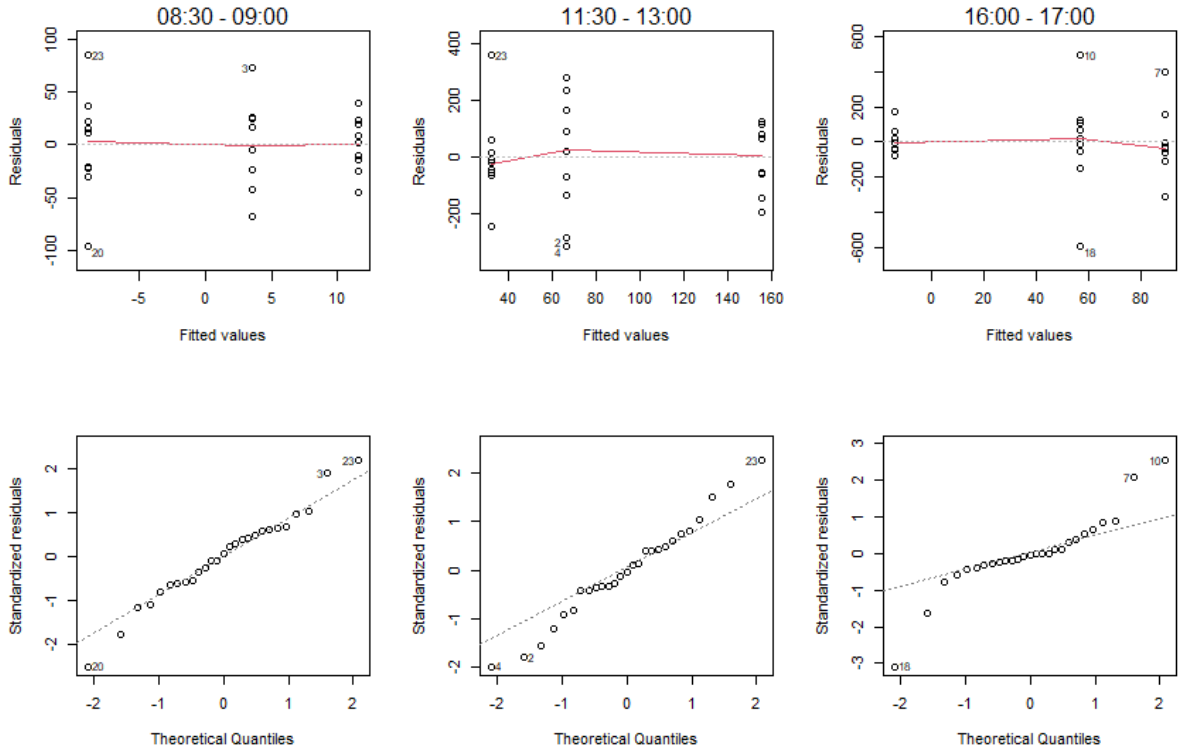

Figure A.7: Residuals plotted against fitted values (upper panel) and quantile-quantile plots (lower panel) for the pairwise differences in stomatal conductance between the two light treatments (high latitude - low latitude). The columns show the three time intervals for point measurements that were considered independent of time within the interval. Nine genotypes (replicates) were included for each of the three types in both light treatments. The plots were used to evaluate the model assumptions of constant variance and normally distributed error terms.

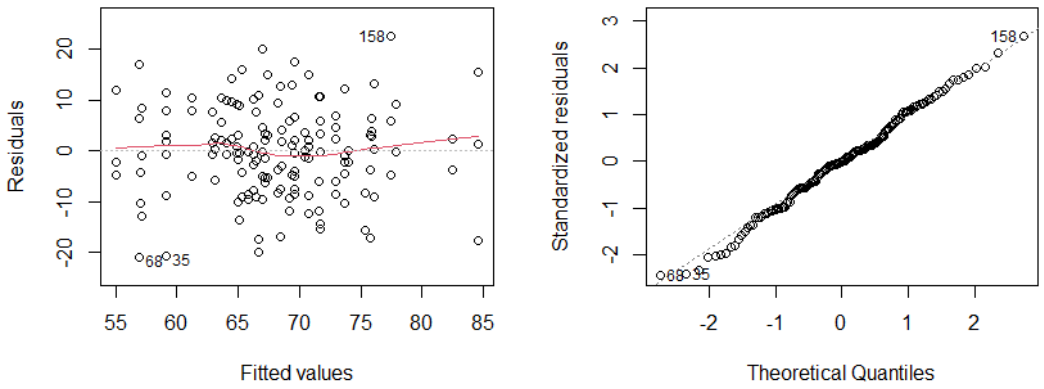

Figure A.8: Residuals plotted against fitted values and quantile-quantile plot for chlorophyll content. Three clones (replicates) were included for each of nine genotypes per type in both light treatments. The plots were used to evaluate the model assumptions of constant variance and normally distributed error terms.

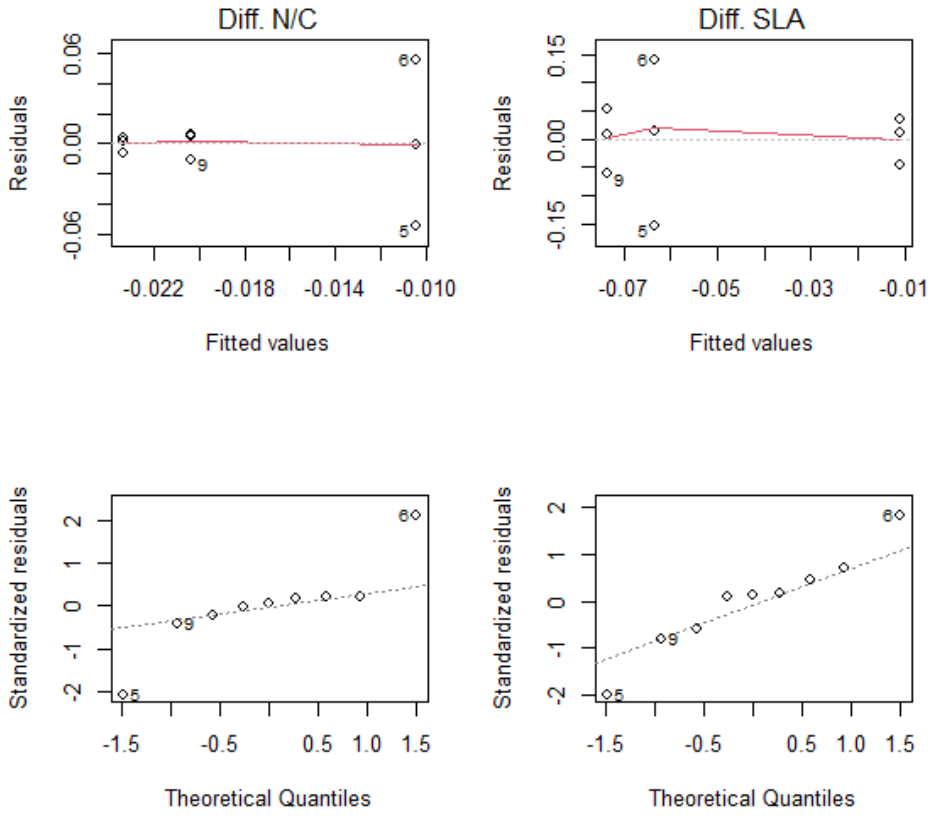

Figure A.9: Residuals plotted against fitted values and quantile-quantile plot for the pairwise differences in the ratio of nitrogen to carbon content (N/C) and specific leaf area (area/dry weight) of leaf blades. Three genotypes (replicates) were included per type. The plots were used to evaluate the model assumptions of constant variance and normally distributed error terms.

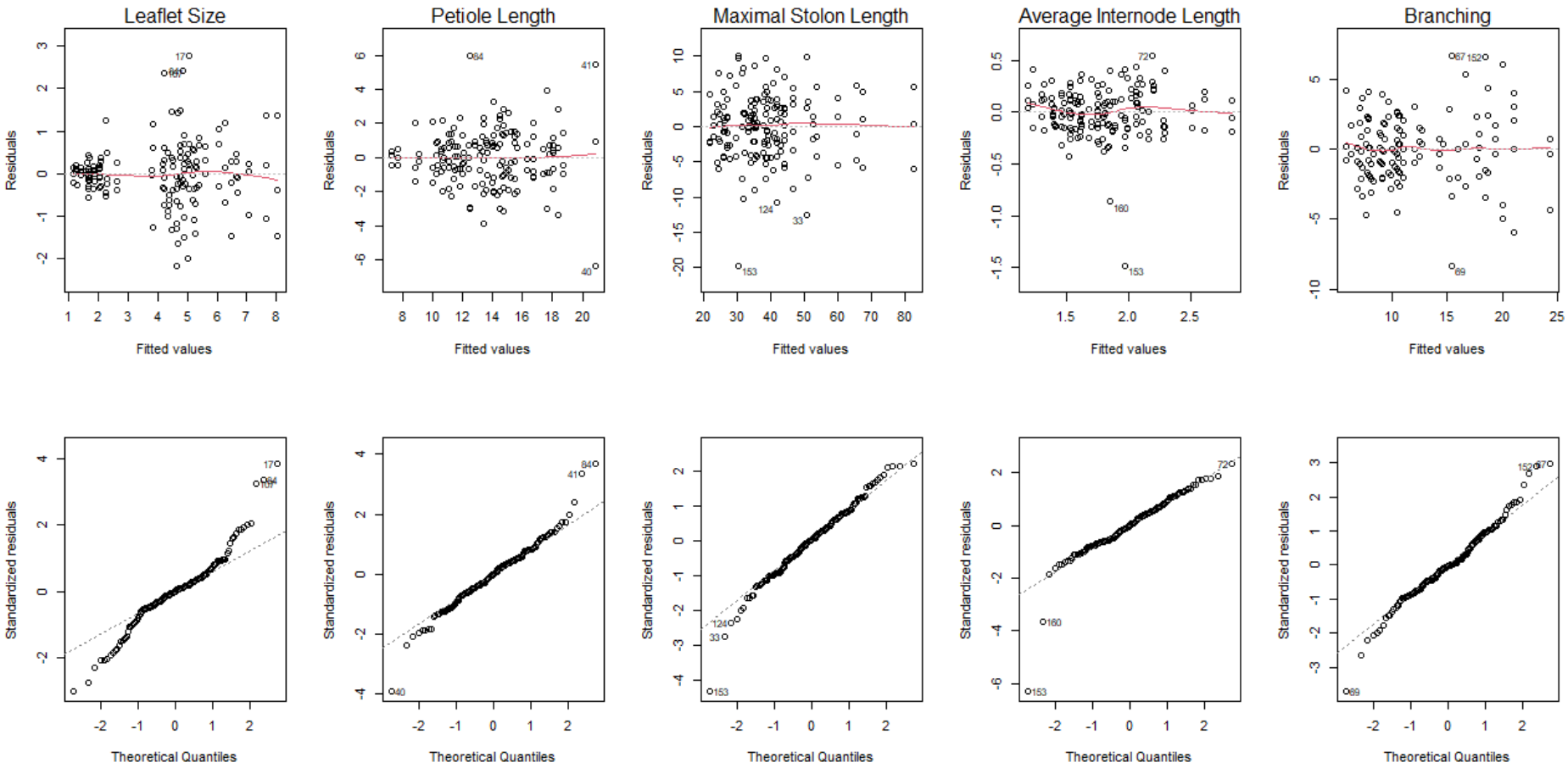

Figure A.10: Residuals plotted against fitted values and quantile-quantile plots for plant growth and architecture variables. Three clones (replicates) were included for each of nine genotypes per type in both light treatments. The plots were used to evaluate the model assumptions of constant variance and normally distributed error terms. Leaflet size (and to some extent petiole length) showed signs of heteroscedasticity and heavy tails in the residuals.

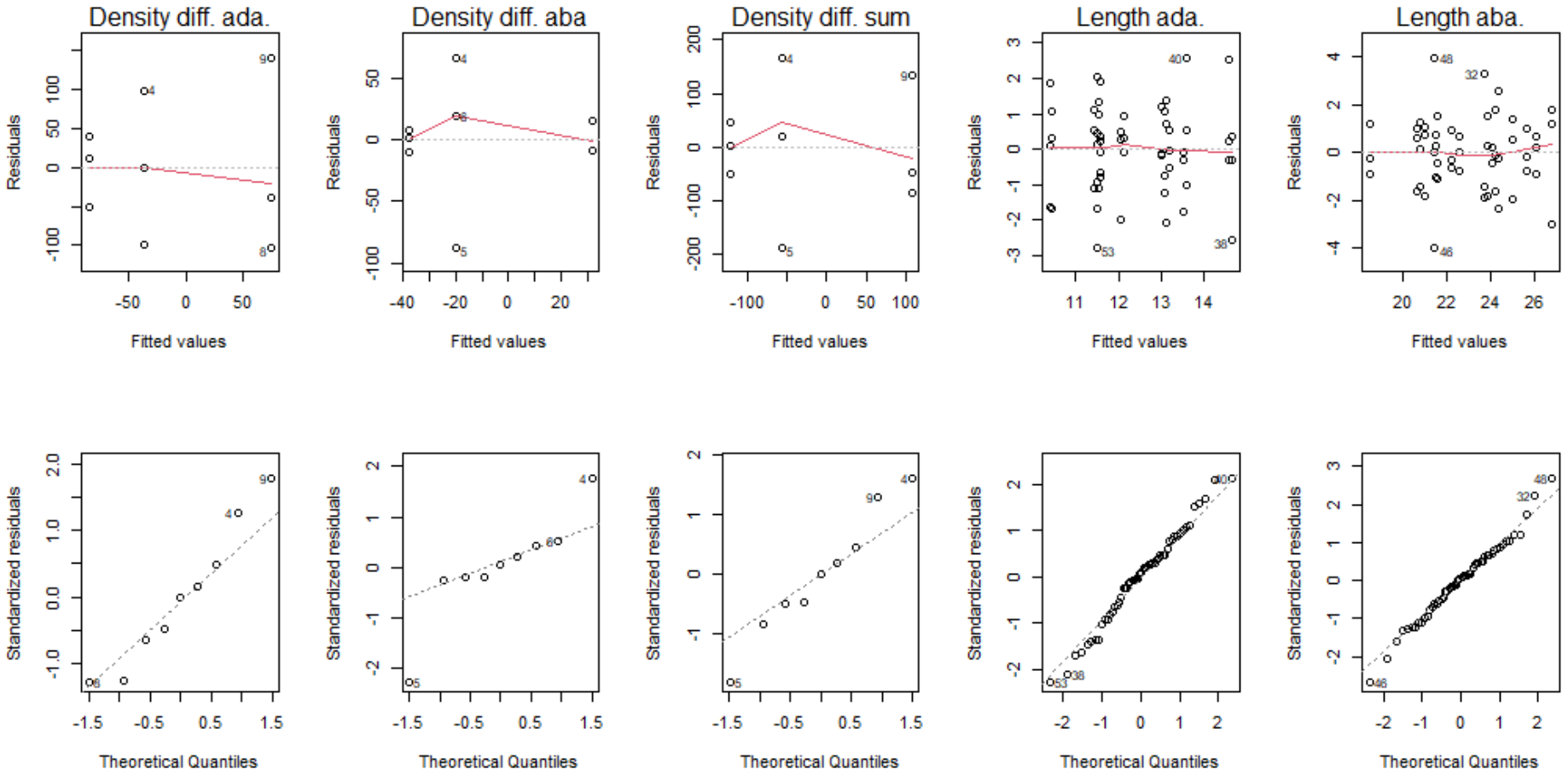

Figure A.11: Residuals plotted against fitted values and quantile-quantile plots for stomatal charachteristics: Stomatal density on both leaf sides and their sum, and length of stomata on each side. Three genotypes (replicates) were included per type for the density measurements, while three randomly selected stomata on each of these were included as replicates for length measurements. The plots were used to evaluate the model assumptions of constant variance and normally distributed error terms.

A.7 Supplementary Results

Table A.6: 95% confidence intervals and R^2-values for the regression coefficients of the least squares regression lines of stomatal conductance as a function of time the first 45 min after white light was turned on (Fig. 14).

Light Treatment	Type	95% C.I. for Regression Coefficient	R^2-value
HL	Finnmark	2.34, 10.5	0.664
	Litago	0.153, 16.0	0.509
	Milkanova	-1.95, 13.3	0.356
LL	Finnmark	3.73, 7.80	0.889
	Litago	2.90, 11.0	0.701
	Milkanova	-0.898, 25.9	0.465

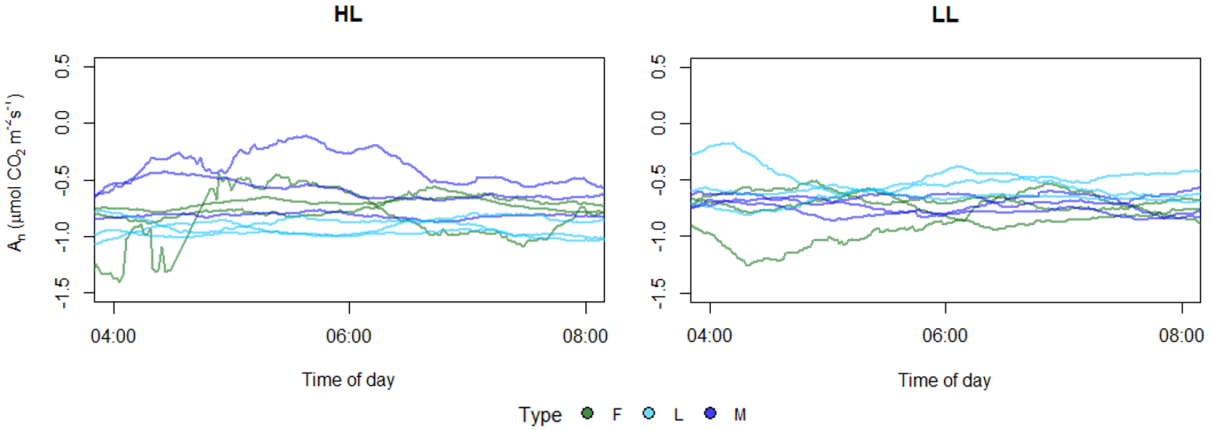

Figure A.12: Respiration at night, given in terms of negative CO_2 assimilation (µmol CO_2 m^{-2} s^{-1}), from the diurnal gas exchange measurements conducted during Experiment 2. The curves shown here are moving averages with periods of 50. F = Finnmark, L = Litago, M = Milkanova, HL = High latitude light treatment, LL = Low latitude light treatment

Table A.7: Results of ANOVA for chlorophyll content. Backwards selection was performed, starting with Model 1, with p-value ≤ 0.05 as selection criteria. The final model is given here. Three clones (replicates) were included for each of nine genotypes per type in both light treatments. Lt = effect of light treatment, T = effect of type, G(T) = effect of genotype in type.

Source	Model	Estimate	F-value	p-value
Lt	$\mu + \tau_i + \beta_j + g_{k(j)} + e_{(ijk)t}$	$\hat{\tau}_{HL}$ = -1.08	2.08	0.151
T			1.03	0.373
G(T)			2.59	**>0.001**

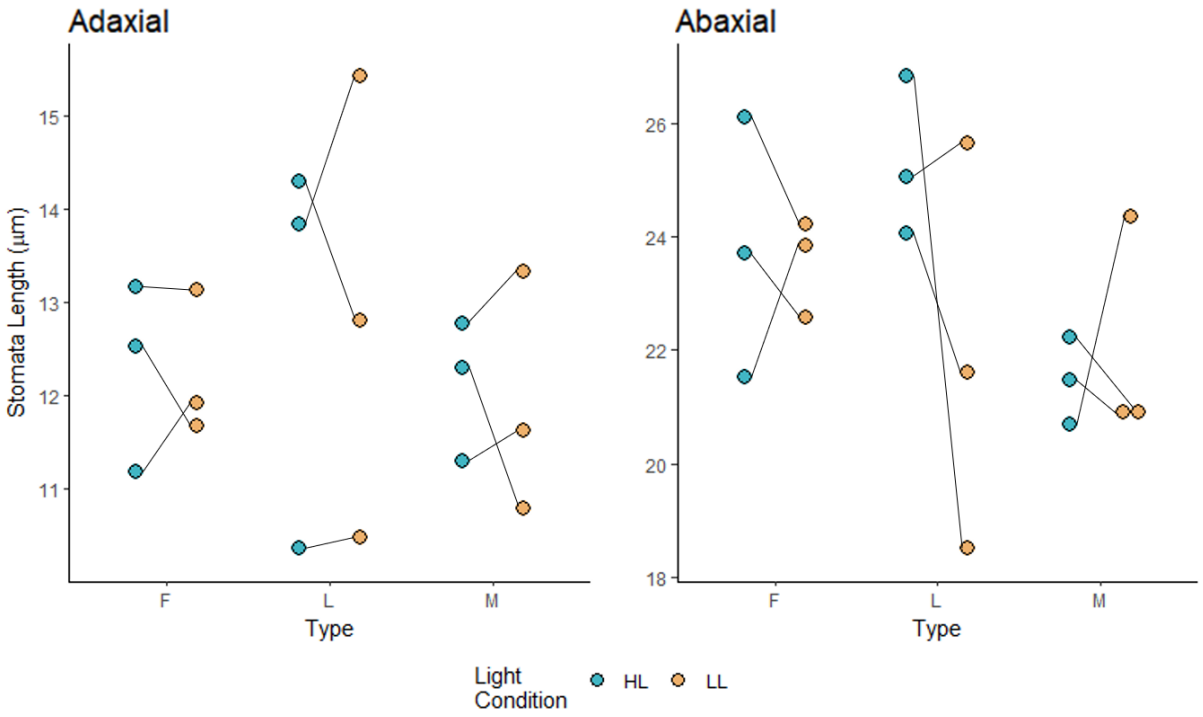

Figure A.13: The points represent genotypes, and are averages of three randomly chosen stomata on the same leaf epidermis imprint. The black lines connect pairs of the same genotype in the two light treatments. Note the different scales. F = Finnmark, L = Litago, M = Milkanova, HL = high latitude, LL = low latitude.

Table A.8: Results of ANOVAs for stomata lengths. Backwards selection was performed, starting with Model 1, with p-value ≤ 0.05 as selection criteria. The final model is given here. Three randomly selected stomata (replicates) from each of three genotypes per type were included per light treatment. Lt = effect of light treatment, T = effect of type, G(T) = effect of genotype in type.

Leaf side	Source	Model	Estimates	F-value	p-value
Adaxial	Lt	$\mu + \tau_i + \beta_j +$	$\hat{\tau}_{HL} = 0.033$	0.0335	0.859
	T	$+g_{k(j)} + e_{(ijk)t}$		0.275	0.768
	G(T)			6.97	**<0.001**
Abaxial	Lt	$\mu + \tau_i + \beta_j +$	$\hat{\tau}_{HL} = 0.504$	0.836	0.396
	T	$+g_{k(j)} + (\tau\beta)_{ij} +$		2.40	0.172
	G(T)	$+(\tau g)_{ik(j)} + e_{(ijk)t}$		1.21	0.361
	Lt x T			0.538	0.765
	Lt x G(T)			5.02	**<0.001**